Chapter 7
Unicycles and Two-Wheel Autonomous Ground Vehicles

Abstract In complement to robotic manipulators, autonomous vehicles form the second large class of robotic systems. In this context, the autonomous or semi-autonomous navigation of unicycle-type and two-wheel vehicles, such as motorcycles, can be significantly improved through electronic control of the their stability properties. This will also allow for precise path following and for dexterous maneuvering. In this chapter, a nonlinear optimal control method is developed for solving the stabilization and path following problem of autonomous two-wheel vehicles. In the presented application examples either the kinematic or the joint kinematic-dynamic of the two-wheel vehicle undergoes approximate linearization around a temporary operating point which is recomputed at each iteration of the control algorithm. The linearization takes place using Taylor series expansion and the computation of the Jacobian matrices of the system's states-space model. For the approximately linearized model of the two-wheel vehicle an H-infinity feedback controller is designed. The computation of the feedback gain of the controller requires the repetitive solution of an algebraic Riccati equation, taking again place at each time-step of the control method. The concept of the control method is that at each time instant the system's state vector is made to converge to the temporary equilibrium, while this equilibrium is shifted towards the reference trajectory. Thus, asymptotically the state vector of the two-wheel vehicle converges to the reference setpoints. Through Lyapunov stability analysis the global asymptotic stability properties of the control method are proven In particular, the chapter treats the following topics: (a) Nonlinear optimal control of robotic unicycles, (b) Flatness-based control of robotic unicycles, and (c) Nonlinear optimal control of autonomous two-wheeled vehicles such as motorcycles.

7.1 Chapter Overview

The present chapter treats the following topics: (a) Nonlinear optimal control of robotic unicycles, (b) Flatness-based control of robotic unicycles, and (c) Nonlinear optimal control of autonomous two-wheeled vehicles such as motorcycles.

G. Rigatos and K. Busawon, *Robotic Manipulators and Vehicles*,
Studies in Systems, Decision and Control 152,
https://doi.org/10.1007/978-3-319-77851-8_7

With reference to (a) the chapter introduces a new control method for feedback control of autonomous robotic vehicles of the unicycle type. The control method consists of a repetitive solution of an H-infinity control problem for the mobile robot, that makes use of a locally linearized model of the robot and takes place at each iteration of the control algorithm. The vehicle's model is locally linearized round its current position through the computation of the associated Jacobian matrices. Using the linearized model of the vehicle an H-infinity feedback control law is computed. The known robustness features of H-infinity control enable to compensate for the errors of the approximate linearization, as well as to eliminate the effects of external perturbations.

With reference to (b) the chapter proposes a differential flatness theory-based implementation of the Kalman Filter (known as Derivative-free nonlinear Kalman Filter) and state estimation-based control for MIMO nonlinear dynamical systems, such as autonomous vehicles. The considered nonlinear filtering scheme which is based on differential flatness theory can be applied to the autonomous vehicle model without the need for calculation of Jacobian matrices, and in general extends the class of MIMO nonlinear systems for which derivative-free Kalman Filtering can be performed. Nonlinear systems such as unicycle-type autonomous vehicles, satisfying the differential flatness property, can be written in the Brunovsky (canonical) form via a transformation of their state variables and control inputs. After transforming the unicycle-type vehicle to the canonical form it is straightforward to apply the standard Kalman Filter recursion.

With reference to (c) the chapter demonstrates that the autonomous or semi-autonomous navigation of two-wheel vehicles, such as motorcycles, can be significantly improved through electronic control of the their stability properties. This will also allow for precise path following and for dexterous maneuvering. Actually, a nonlinear optimal control method is developed once again, for solving the stabilization and path following problem of autonomous motorcycles. The joint kinematic and dynamic model of the motorcycle undergoes approximate linearization around a temporary operating point which is recomputed at each iteration of the control algorithm. The linearization takes place using Taylor series expansion and the computation of the Jacobian matrices of the system's states-space model. For the approximately linearized model of the motorcycle an H-infinity feedback controller is designed. The computation of the feedback gain of the controller requires the repetitive solution of an algebraic Riccati equation, taking again place at each time-step of the control method. The concept of the control method is that at each time instant the autonomous motorcycle's state vector is made to converge to the temporary equilibrium, while this equilibrium is shifted towards the reference trajectory. Thus, asymptotically the state vector of the motorcycle converges to the reference setpoints. In all cases (a)–(c) the global asymptotic stability properties of the control method are proven through Lyapunov analysis.

7.2 Nonlinear Optimal Control of the Robotic Unicycle

7.2.1 Outline

Nonlinear and embedded control and autonomous navigation of robotic vehicles is of primary importance for the automotive industry. By succeeding motion control of the vehicle, safety in driving can be improved while other several practical problems, such as lane keeping and maneuvering or parallel parking can be solved [206, 207, 223, 278, 281, 425, 569, 574]. Up to now several research results have been developed to enable the steering control and autonomous navigation of vehicles. The developed methods are based on nonlinear control, such as differential geometry and differential flatness theory approaches as well as on Lyapunov stability theory [38, 90, 100, 262, 343, 486, 604]. In this section a new solution to the problem of autonomous vehicle navigation is given, using a linearization scheme together with H_∞ robust control theory [450].

The kinematic model of a unicycle robotic vehicle is considered as a case study, however the proposed approach can be also applied to other types of vehicles (such as four wheel vehicles, heavy duty vehicles, articulated vehicles etc.). Actually the present section proposes the application of an approximate linearization scheme for the kinematic model of the unicycle robotic vehicle. The linearization makes use of Taylor series expansion around the vehicle's current position. To perform this linearization the computation of Jacobian matrices is needed while the induced linearization error is treated as a disturbance. For the linearized equivalent of the vehicle's model an H_∞ feedback control scheme is developed. The formulation of the H_∞ control problem is based on the minimization of a quadratic cost function that comprises both the disturbance and the control input effects. The disturbance tries to maximize the cost function while the control signal tries to minimize it, within a min-max differential game.

Comparing to nonlinear feedback control approaches which rely on exact linearization (as the ones based on differential flatness theory and analyzed in [450, 452, 457]) the proposed H_∞ control scheme is assessed as follows: (i) it uses an approximate linearization approach of the vehicle's dynamic or kinematic model which does not follow the elaborated transformations (diffeomorphisms) of the exact linearization methods, (ii) it introduces additional disturbance error which is due to the approximate linearization of the system dynamics coming from the application of Taylor series expansion, (iii) it requires the computation of Jacobian matrices, (iv) unlike exact feedback linearization, the H_∞ control term has to compensate not only for modelling uncertainties and external disturbances but needs also to annihilate the effects of the cumulative linearization error, (v) the H_∞ control approach follows optimal control methods for the computation of the control signal, thus achieving accurate tracking of reference setpoints under moderate variations of the control input.

7.2.2 *Linearization of the Robotic Vehicle's Kinematic Model*

7.2.2.1 Approaches in Control of Nonlinear Robotic Vehicles

Motion control of unmanned vehicles is a nonlinear control problem. One can distinguish three main approaches in the design of nonlinear control systems: (i) control and filtering based on global linearization methods, (ii) control and filtering based on asymptotic linearization methods, (iii) Lyapunov methods.

As far as approach (i) is concerned, that is methods of global linearization, one can classify there methods for the transformation of nonlinear vehicles dynamics into equivalent linear state space form. For the linear equivalent forms of the vehicles dynamics one can design feedback controllers and can solve the problem of state estimation (filtering). In this area one can consider methods based on differential flatness theory and methods based on Lie algebra. These approaches avoid approximation errors in modelling and arrive at controllers of elevated precision and robustness, In this area, one can also distinguish a new nonlinear filtering method (Derivative-free nonlinear Kalman Filter) which is more precise and computationally faster than other nonlinear estimation approaches [450].

As far as approach (ii) is concerned, that is methods of asymptotic linearization, the focus is on robust and adaptive control with the use of a decomposition of the vehicles dynamics into a set of linear local models. One can pursue solutions to the problem of nonlinear control, relying on local linear models (around linearization points). For such systems one can select the parameters of the local controllers by following linear feedback controller design methods. These controllers achieve asymptotically, that is in the course of time, the compensation of the nonlinear system dynamics and the stabilization of the feedback control loops. In this research direction several results have been obtained about a new nonlinear H-infinity control method, which is based on the local and approximate linearization of the vehicles dynamics and which makes use of the computation of Jacobian matrices.

As far as approach (iii) is concerned, that is Lyapunov theory-based nonlinear control methods one comes against problems of minimization of the Lyapunov functions so as to compute control signals for nonlinear vehicle dynamics. For the development of Lyapunov-type controllers one can either exploit a model of the vehicle's dynamics, or can avoid completely the use of such a model as in the case of adaptive control. In the latter case, the vehicles dynamics is completely unknown and can be approximated by adaptive algorithms which are suitably designed so as to assure the stability and robustness of the control loop.

7.2.3 *Linearization of the Unicycle Robot Through Taylor Series Expansion*

A unicycle autonomous robotic vehicle is considered, as shown in Fig. 7.1. Its kinematic model is given by

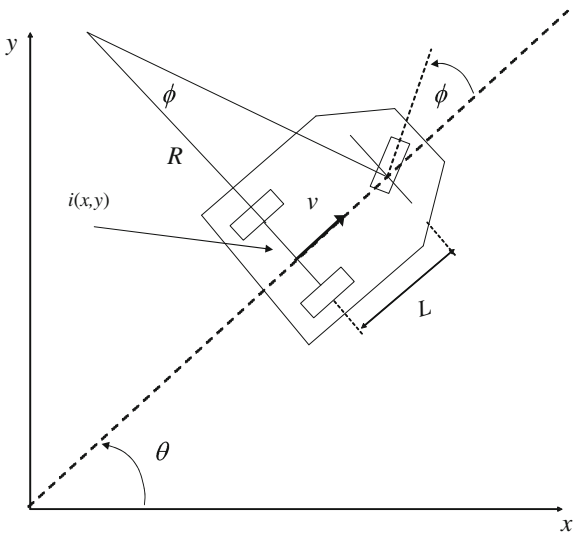

Fig. 7.1 The model of the autonomous robotic vehicle (cart-like vehicle)

$$\begin{pmatrix} \dot{x} \\ \dot{y} \\ \dot{\theta} \end{pmatrix} = \begin{pmatrix} cos(\theta) & 0 \\ sin(\theta) & 0 \\ 0 & 1 \end{pmatrix} \cdot \begin{pmatrix} v \\ \omega \end{pmatrix} \tag{7.1}$$

where x, y are the cartesian coordinates of the robot's center of gravity and θ is its orientation angle. Input v is the vehicle's linear velocity and ω is the vehicle's angular velocity for rotations round its transversal axis.

Considering linearization of the model round the current position of the robot and round the velocity value $v(t - T_s)$, where T_S is the sampling period, the Jacobian matrices of the robotic model are:

$$A = \begin{pmatrix} 0 & 0 & -v(t - T_s) \cdot sin(\theta) \\ 0 & 0 & v(t - T_s) \cdot cos(\theta) \\ 0 & 0 & 0 \end{pmatrix} \tag{7.2}$$

$$B = \begin{pmatrix} cos(\theta) & 0 \\ sin(\theta) & 0 \\ 0 & 1 \end{pmatrix} \tag{7.3}$$

The state vector of the robotic vehicle is denoted as $\mathbf{x} = [\mathbf{x}, \mathbf{y}, \boldsymbol{\theta}]^{\mathbf{T}}$ while the input vector is denoted as $u = [v, w]^T$. After linearization around its current position, the robot's kinematic model is written as

$$\dot{x} = Ax + Bu + d_1 \tag{7.4}$$

Parameter d_1 stands for the linearization error in the robot's kinematic model appearing in Eq. (7.4). The desirable trajectory of the robot is denoted by $\mathbf{x_d} = [\mathbf{x_d}, \mathbf{y_d}, \boldsymbol{\theta}_\mathbf{d}]$. Tracking of this trajectory is achieved after applying the control input u^*. At every time instant the control input u^* is assumed to differ from the control input u appearing in Eq. (7.4) by an amount equal to Δu, that is $u^* = u + \Delta u$

$$\dot{x}_d = Ax_d + Bu^* + d_2 \tag{7.5}$$

The dynamics of the controlled system described in Eq. (7.4) can be also written as

$$\dot{x} = Ax + Bu + Bu^* - Bu^* + d_1 \tag{7.6}$$

and by denoting $d_3 = -Bu^* + d_1$ as an aggregate disturbance term one obtains

$$\dot{x} = Ax + Bu + Bu^* + d_3 \tag{7.7}$$

By subtracting Eq. (7.5) from Eq. (7.7) one has

$$\dot{x} - \dot{x}_d = A(x - x_d) + Bu + d_3 - d_2 \tag{7.8}$$

By denoting the tracking error as $e = x - x_d$ and the aggregate disturbance term as $\tilde{d} = d_3 - d_2$, the tracking error dynamics becomes

$$\dot{e} = Ae + Bu + \tilde{d} \tag{7.9}$$

The above linearized form of the robotic model can be efficiently controlled after applying an H-infinity feedback control scheme.

7.2.4 The Nonlinear H-Infinity Control

7.2.4.1 Mini-Max Control and Disturbance Rejection

The initial nonlinear system is assumed to be in the form

$$\dot{x} = f(x, u) \;\; x \in R^n, \;\; u \in R^m \tag{7.10}$$

Linearization of the system (autonomous vehicle) is performed at each iteration of the control algorithm round its present operating point $(x^*, u^*) = (x(t), u(t - T_s))$. The linearized equivalent of the system is described by

$$\dot{x} = Ax + Bu + L\tilde{d} \;\; x \in R^n, \;\; u \in R^m, \;\; \tilde{d} \in R^q \tag{7.11}$$

where matrices A and B are obtained from the computation of the Jacobians

$$A = \begin{pmatrix} \frac{\partial f_1}{\partial x_1} & \frac{\partial f_1}{\partial x_2} & \cdots & \frac{\partial f_1}{\partial x_n} \\ \frac{\partial f_2}{\partial x_1} & \frac{\partial f_2}{\partial x_2} & \cdots & \frac{\partial f_2}{\partial x_n} \\ \cdots & \cdots & \cdots & \cdots \\ \frac{\partial f_n}{\partial x_1} & \frac{\partial f_n}{\partial x_2} & \cdots & \frac{\partial f_n}{\partial x_n} \end{pmatrix} |_{(x^*,u^*)} \tag{7.12}$$

$$B = \begin{pmatrix} \frac{\partial f_1}{\partial u_1} & \frac{\partial f_1}{\partial u_2} & \cdots & \frac{\partial f_1}{\partial u_m} \\ \frac{\partial f_2}{\partial u_1} & \frac{\partial f_2}{\partial u_2} & \cdots & \frac{\partial f_2}{\partial u_m} \\ \cdots & \cdots & \cdots & \cdots \\ \frac{\partial f_n}{\partial u_1} & \frac{\partial f_n}{\partial u_2} & \cdots & \frac{\partial f_n}{\partial u_m} \end{pmatrix} |_{(x^*,u^*)} \tag{7.13}$$

and vector $\tilde{d}$ denotes disturbance terms due to linearization errors. The problem of disturbance rejection for the linearized model that is described by

$$\begin{gathered} \dot{x} = Ax + Bu + Ld \\ y = Cx \end{gathered} \tag{7.14}$$

where $x \in R^n$, $u \in R^m$, $\tilde{d} \in R^q$ and $y \in R^p$, cannot be handled efficiently if the classical LQR control scheme is applied. This is because of the existence of the perturbation term d. The disturbance term d apart from modeling (parametric) uncertainty and external perturbation terms can also represent noise terms of any distribution.

As analyzed in previous applications of the H_∞ control approach, a feedback control scheme is designed for trajectory tracking by the system's state vector and simultaneous disturbance rejection, considering that the disturbance affects the system in the worst possible manner. The disturbances' effects are incorporated in the following quadratic cost function:

$$\begin{gathered} J(t) = \frac{1}{2}\int_0^T [y^T(t)y(t) + \\ + ru^T(t)u(t) - \rho^2 \tilde{d}^T(t)\tilde{d}(t)]dt, \quad r, \rho > 0 \end{gathered} \tag{7.15}$$

As pointed out in previous sections, the significance of the negative sign in the cost function's term that is associated with the perturbation variable $\tilde{d}(t)$ is that the disturbance tries to maximize the cost function $J(t)$ while the control signal $u(t)$ tries to minimize it. The physical meaning of the relation given above is that the control signal and the disturbances compete to each other within a min-max differential game. This problem of min-max optimization can be written as

$$min_u max_{\tilde{d}} J(u, \tilde{d}) \tag{7.16}$$

The objective of the optimization procedure is to compute a control signal $u(t)$ which can compensate for the worst possible disturbance, that is externally imposed to the unicycle vehicle. However, the solution to the min-max optimization problem is directly related to the value of the parameter ρ. This means that there is an upper bound in the disturbances magnitude that can be annihilated by the control signal.

7.2.4.2 H-Infinity Feedback Control

For the linearized system given by Eq. (7.14) the cost function of Eq. (7.15) is defined, where the coefficient r determines the penalization of the control input and the weight coefficient ρ determines the reward of the disturbances' effects. It is assumed that:

As in previous applications of the H-infinity control method, it is assumed that (i) The energy that is transferred from the disturbances signal $d(t)$ is bounded, that is $\int_0^\infty \tilde{d}^T(t)\tilde{d}(t)dt < \infty$, (ii) matrices $[AB]$ and $[AL]$ are stabilizable, (iii) matrix $[AC]$ is detectable. Then, the optimal feedback control law is given by

$$u(t) = -Kx(t) \tag{7.17}$$

with

$$K = \frac{1}{r}B^T P \tag{7.18}$$

where P is a positive semi-definite symmetric matrix which is obtained from the solution of the Riccati equation

$$A^T P + PA + Q - P(\frac{1}{r}BB^T - \frac{1}{2\rho^2}LL^T)P = 0 \tag{7.19}$$

where Q is also a positive definite symmetric matrix. The worst case disturbance is given by $\tilde{d}(t) = \frac{1}{\rho^2}L^T Px(t)$.

7.2.5 Lyapunov Stability Analysis

Through Lyapunov stability analysis it will be shown that the proposed nonlinear control scheme for the unicycle vehicle assures H_∞ tracking performance, and that in case of bounded disturbance terms asymptotic convergence to the reference setpoints is achieved. The tracking error dynamics for the robotic vehicle is written in the form

$$\dot{e} = Ae + Bu + L\tilde{d} \tag{7.20}$$

where in the unicycle robot's application example $L = I \in R^3$ with I being the identity matrix. The following Lyapunov function is considered

$$V = \frac{1}{2}e^T Pe \tag{7.21}$$

where $e = x - x_d$ is the tracking error. By differentiating with respect to time one obtains

$$\begin{gathered}\dot{V} = \tfrac{1}{2}\dot{e}^T Pe + \tfrac{1}{2}eP\dot{e} \Rightarrow \\ \dot{V} = \tfrac{1}{2}[Ae + Bu + L\tilde{d}]^T P + \tfrac{1}{2}e^T P[Ae + Bu + L\tilde{d}] \Rightarrow\end{gathered} \tag{7.22}$$

$$\begin{gathered}\dot{V} = \tfrac{1}{2}[e^T A^T + u^T B^T + \tilde{d}^T L^T]Pe + \\ + \tfrac{1}{2}e^T P[Ae + Bu + L\tilde{d}] \Rightarrow\end{gathered} \tag{7.23}$$

$$\begin{gathered}\dot{V} = \tfrac{1}{2}e^T A^T Pe + \tfrac{1}{2}u^T B^T Pe + \tfrac{1}{2}\tilde{d}^T L^T Pe + \\ \tfrac{1}{2}e^T PAe + \tfrac{1}{2}e^T PBu + \tfrac{1}{2}e^T PL\tilde{d}\end{gathered} \tag{7.24}$$

The previous equation is rewritten as

$$\begin{gathered}\dot{V} = \tfrac{1}{2}e^T(A^T P + PA)e + \left(\tfrac{1}{2}u^T B^T Pe + \tfrac{1}{2}e^T PBu\right) + \\ + \left(\tfrac{1}{2}\tilde{d}^T L^T Pe + \tfrac{1}{2}e^T PL\tilde{d}\right)\end{gathered} \tag{7.25}$$

Assumption: For given positive definite matrix Q and coefficients r and ρ there exists a positive definite matrix P, which is the solution of the following matrix equation

$$A^T P + PA = -Q + P\left(\tfrac{1}{r}BB^T - \tfrac{1}{2\rho^2}LL^T\right)P \tag{7.26}$$

Moreover, the following feedback control law is applied to the system

$$u = -\tfrac{1}{r}B^T Pe \tag{7.27}$$

By substituting Eq. (7.26) and Eq. (7.27) one obtains

$$\begin{gathered}\dot{V} = \tfrac{1}{2}e^T\left[-Q + P\left(\tfrac{1}{r}BB^T - \tfrac{1}{2\rho^2}LL^T\right)P\right]e + \\ + e^T PB\left(-\tfrac{1}{r}B^T Pe\right) + e^T PL\tilde{d} \Rightarrow\end{gathered} \tag{7.28}$$

$$\begin{gathered}\dot{V} = -\tfrac{1}{2}e^T Qe + \left(\tfrac{1}{r}PBB^T Pe - \tfrac{1}{2\rho^2}e^T PLL^T\right)Pe \\ -\tfrac{1}{r}e^T PBB^T Pe + e^T PL\tilde{d}\end{gathered} \tag{7.29}$$

which after intermediate operations gives

$$\dot{V} = -\tfrac{1}{2}e^T Qe - \tfrac{1}{2\rho^2}e^T PLL^T Pe + e^T PL\tilde{d} \tag{7.30}$$

or, equivalently

$$\begin{gathered}\dot{V} = -\tfrac{1}{2}e^T Qe - \tfrac{1}{2\rho^2}e^T PLL^T Pe + \\ + \tfrac{1}{2}e^T PL\tilde{d} + \tfrac{1}{2}\tilde{d}^T L^T Pe\end{gathered} \tag{7.31}$$

Lemma: The following inequality holds

$$\frac{1}{2}e^T L\tilde{d} + \frac{1}{2}\tilde{d}L^T Pe - \frac{1}{2\rho^2}e^T PLL^T Pe \leq \frac{1}{2}\rho^2\tilde{d}^T\tilde{d} \tag{7.32}$$

Proof: The binomial $(\rho\alpha - \frac{1}{\rho}b)^2$ is considered. Expanding the left part of the above inequality one gets

$$\begin{gathered}\rho^2a^2 + \frac{1}{\rho^2}b^2 - 2ab \geq 0 \Rightarrow \frac{1}{2}\rho^2a^2 + \frac{1}{2\rho^2}b^2 - ab \geq 0 \Rightarrow \\ ab - \frac{1}{2\rho^2}b^2 \leq \frac{1}{2}\rho^2a^2 \Rightarrow \frac{1}{2}ab + \frac{1}{2}ab - \frac{1}{2\rho^2}b^2 \leq \frac{1}{2}\rho^2a^2\end{gathered} \tag{7.33}$$

The following substitutions are carried out: $a = \tilde{d}$ and $b = e^T PL$ and the previous relation becomes

$$\frac{1}{2}\tilde{d}^T L^T Pe + \frac{1}{2}e^T PL\tilde{d} - \frac{1}{2\rho^2}e^T PLL^T Pe \leq \frac{1}{2}\rho^2\tilde{d}^T\tilde{d} \tag{7.34}$$

Equation (7.34) is substituted in Eq. (7.31) and the inequality is enforced, thus giving

$$\dot{V} \leq -\frac{1}{2}e^T Qe + \frac{1}{2}\rho^2\tilde{d}^T\tilde{d} \tag{7.35}$$

Equation (7.35) shows that the H_∞ tracking performance criterion is satisfied. The integration of $\dot{V}$ from 0 to T gives

$$\begin{gathered}\int_0^T \dot{V}(t)dt \leq -\frac{1}{2}\int_0^T ||e||_Q^2 dt + \frac{1}{2}\rho^2\int_0^T ||\tilde{d}||^2 dt \Rightarrow \\ 2V(T) + \int_0^T ||e||_Q^2 dt \leq 2V(0) + \rho^2\int_0^T ||\tilde{d}||^2 dt\end{gathered} \tag{7.36}$$

Moreover, if there exists a positive constant $M_d > 0$ such that

$$\int_0^\infty ||\tilde{d}||^2 dt \leq M_d \tag{7.37}$$

then one gets

$$\int_0^\infty ||e||_Q^2 dt \leq 2V(0) + \rho^2 M_d \tag{7.38}$$

Thus, the integral $\int_0^\infty ||e||_Q^2 dt$ is bounded. Moreover, $V(T)$ is bounded and from the definition of the Lyapunov function V in Eq. (7.21) it becomes clear that $e(t)$ will be also bounded since $e(t) \in \Omega_e = \{e | e^T Pe \leq 2V(0) + \rho^2 M_d\}$. According to the above and with the use of Barbalat's Lemma one obtains $lim_{t\to\infty} e(t) = 0$.

7.2.6 Simulation Tests

The performance of the proposed nonlinear H_∞ control scheme is tested is two examples: (i) when the mobile robot tracks a reference trajectory, (ii) when the unicycle robot performs the automated parallel parking task. In both cases the performance of the proposed controller was satisfactory, with minimum tracking error and fast

convergence to the reference setpoints. In the computation of the reference path, the coordinates of the reference trajectory in the 2D-plane (x_d, y_d) have been used, while the desirable steering angle has been computed by $\theta_d = tan^{-1}(\dot{y}_d/\dot{x}_d)$. The obtained results are depicted in Figs. 7.2, 7.3 and 7.4.

The tracking performance of the control method is shown in Table 7.1. It can be observed that the tracking error for all state variables of the unicycle robot was extremely small. Besides, in the simulation diagrams one can note the excellent transient performance of the control algorithm, which means that convergence to the

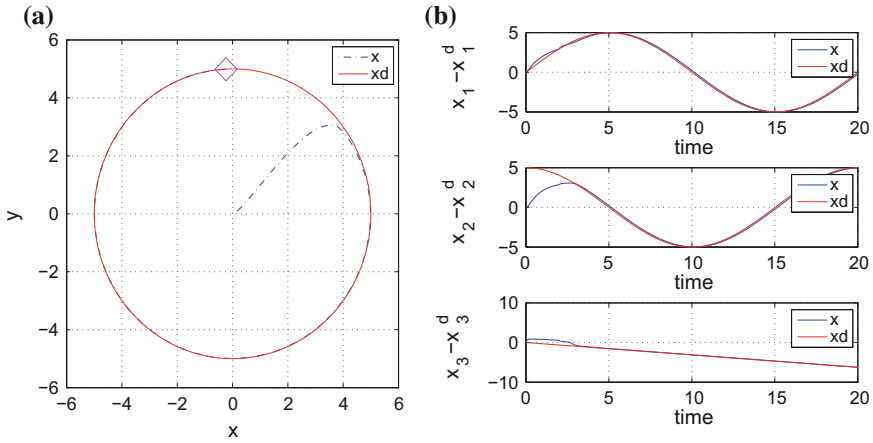

Fig. 7.2 **a** Plot of the circular $x - y$ trajectory followed by the mobile robot, **b** convergence of the robot's state variables $x_1 = x$, $x_2 = y$ and $x_3 = \theta$ to the associated reference setpoints

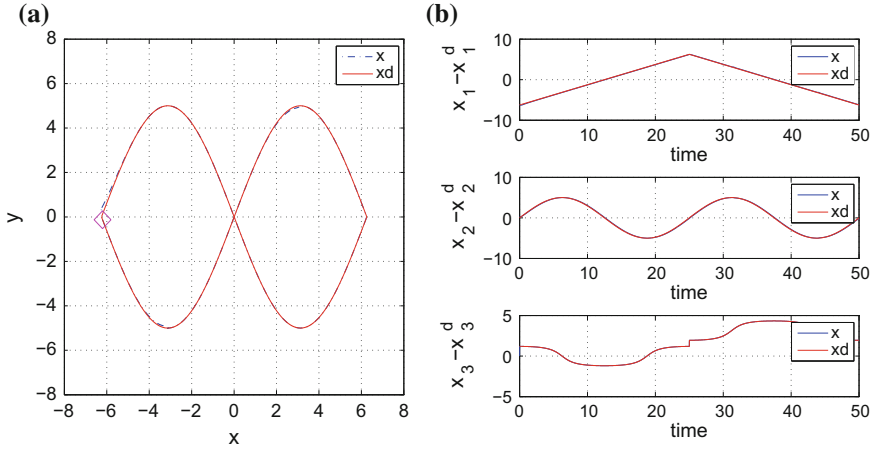

Fig. 7.3 **a** Plot of the eight-shaped $x - y$ trajectory followed by the mobile robot, **b** convergence of the robot's state variables $x_1 = x$, $x_2 = y$ and $x_3 = \theta$ to the associated reference setpoints

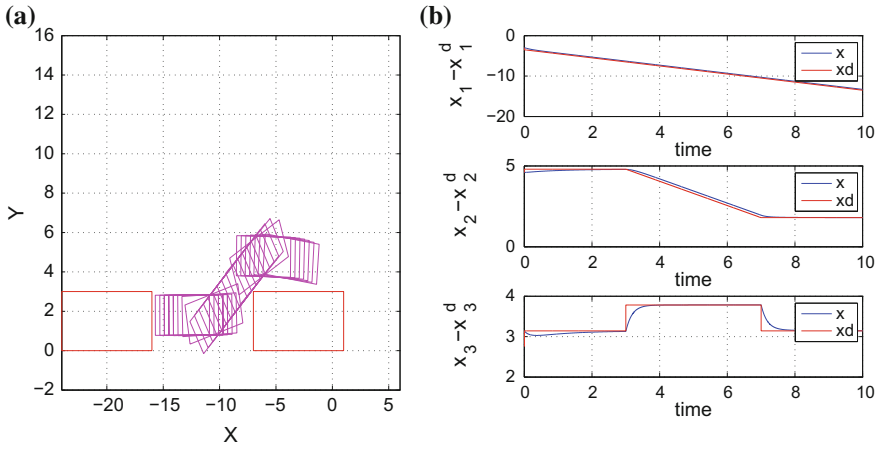

Fig. 7.4 **a** Plot of the $x - y$ trajectory followed by the mobile robot in case of the parallel parking maneuver, **b** convergence of the robot's state variables $x_1 = x, x_2 = y$ and $x_3 = \theta$ to the associated reference setpoints

Table 7.1 Tracking RMSE in the disturbance-free case

	$RMSE_x$	$RMSE_y$	$RMSE_\theta$
Path_1	$36.00 \cdot 10^{-4}$	$39.00 \cdot 10^{-4}$	$10.00 \cdot 10^{-4}$
Path_2	$7.90 \cdot 10^{-4}$	$12.00 \cdot 10^{-4}$	$2.40 \cdot 10^{-4}$

reference path was succeeded in a smooth manner, while also avoiding overshoot and oscillations.

It is pointed out that the errors and disturbances that affect the proposed control method are as follows: (i) linearization errors due to the truncation of higher order terms in the Taylor series expansion of the vehicle's nonlinear model, (ii) external perturbations that may affect the vehicle's motion. H-infinity control aims at providing maximum robustness to this kind of modeling errors and disturbances, and this is achieved through the appropriate selection of the attenuation coefficient ρ which appears in the associated Riccati equation. Actually, the minimum value of ρ for which there exists a solution for the algebraic Riccati equation (in the form of a positive definite symmetric matrix P) is the one that provides the control loop with maximum robustness. The above have been explained in Sect. 3.3 of manuscript.

Moreover, it is pointed out that the control method that is presented in this section and which is based on nonlinear H-infinity control theory can be compared against global linearization methods, e.g. those based on differential flatness theory and against Lyapunov-based methods (used by adaptive control schemes) [450, 452, 457]. As a general remark it can be stated that the nonlinear H-infinity control, yet conceptually more simple than the other two control approaches, is a reliable and efficient solution for the problem of autonomous vehicles' control. Besides,by avoiding

the intuitive definition of linearizing outputs and the elaborated computations associated with state variables' transformations met in global linearization-based control schemes, the nonlinear optimal control approach appears to be advantageous.

7.3 Flatness-Based Control of the Robotic Unicycle

7.3.1 Outline

In this section, using differential flatness theory, the nonlinear dynamics of the vehicle (e.g. the UGV of Fig. 7.5) is first subject to a linearization transformation. This makes possible (i) to design an efficient control law for trajectories tracking, and (ii) to apply to the nonlinear system a filtering method that it is based on the standard Kalman Filter recursion. Unlike the Extended Kalman Filter (EKF), the proposed filtering method provides estimates of the state vector of the UGV without the need for derivatives and Jacobians calculation. By avoiding linearization approximations, the proposed derivative-free nonlinear Kalman filtering method improves the accuracy of estimation of the system state variables, and results in smooth control signal variations and in minimization of the tracking error of the associated control loop.

Filtering-based state estimation for unmanned ground vehicles (UGVs) is a significant topic because it enables their accurate localization and autonomous navigation [45]. For nonlinear systems such as UGVs, and under the assumption of Gaussian noise, the Extended Kalman Filter (EKF) is frequently applied for estimating the non-measurable state variables through the processing of input and output sequences or

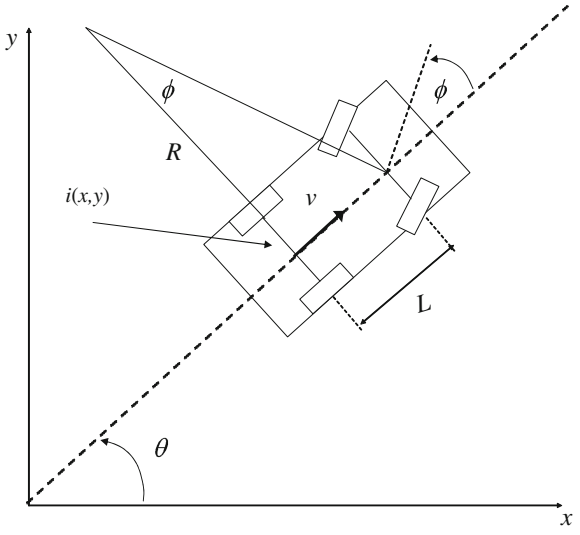

Fig. 7.5 The model of the 4-wheel autonomous vehicle (car-like vehicle) is approximated by that of the unicycle at moderate speeds

for obtaining estimates of the state vector through the fusion of measurements coming from various sensors [33, 190, 222, 359]. The Extended Kalman Filter is based on linearization of the system dynamics using a first order Taylor expansion [431, 432, 439, 445, 449, 601]. Although EKF is efficient in several estimation and fusion problems, it is characterized by cumulative errors due to the local linearization assumption and this may affect the accuracy of the UGV's motion estimation or even risk the stability of the UGV state estimation-based control loop.

The present section extends the results of [415, 433] towards nonlinear dynamical systems, such as UGVs, which are described by multi-input multi-output (MIMO) models. Actually, the section's results are applicable to differentially flat MIMO nonlinear dynamical systems which after employing the differential flatness theory can be written in the Brunovksy (canonical) form [254, 322]. Simulation experiments on the problem of autonomous navigation of a unicycle robotic vehicle are provided to test the performance of the proposed derivative-free Kalman Filter.

7.3.2 Application of Derivative-Free Kalman Filtering to UGVs

7.3.2.1 Kinematic Models for Autonomous Vehicles

The proposed method of derivative-free nonlinear Kalman Filtering (DKF) for MIMO nonlinear systems will be analyzed through an application example. Once again the kinematic model of a UGV (unicycle robotic vehicle) is considered. This is given by

$$\begin{aligned} \dot{x} &= vcos(\theta) \\ \dot{y} &= vsin(\theta) \\ \dot{\theta} = \omega &= \tfrac{v}{L} tan(\phi) \end{aligned} \tag{7.39}$$

where $v(t)$ is the velocity of the vehicle, L is the distance between the front and the rear wheel axis of the vehicle, θ is the angle between the transversal axis of the vehicle and axis OX, and ϕ is the angle of the steering wheel with respect to the transversal axis of the vehicle. As shown in previous sections, the position of such a vehicle is described by the coordinates (x, y) of the center of its rear axis and its orientation is given by the angle θ between the x-axis and the axis of the direction of the vehicle. The steering angle ϕ and the speed v are considered to be the inputs of the system.

The problem of control of autonomous ground vehicles (AGVs) of the unicycle-type is considered once more. The position of such a vehicle is described by the coordinates (x, y) of the center of its rear axis and its orientation is given by the angle θ between the x-axis and the axis of the direction of the vehicle. The steering angle ϕ and the speed u are considered to be the inputs of the system. The kinematic model of autonomous vehicles can be expressed in the general form [415]

$$\begin{pmatrix} \dot{x} \\ \dot{y} \\ \dot{\theta} \end{pmatrix} = \begin{pmatrix} cos(\theta) & 0 \\ sin(\theta) & 0 \\ 0 & 1 \end{pmatrix} \cdot \begin{pmatrix} v(t) \\ v(t)\rho(t) \end{pmatrix} \tag{7.40}$$

where (x, y) are the coordinates of the center of the vehicle's rear wheels axis, $v(t)$ is the velocity of the vehicle, and θ is the angle between the transversal axis of the vehicle and axis OX, while $\rho(t) = 1/r(t)$ is the curvature of the robot's path. The autonomous vehicle is a nonholonomic system. Nonholonomic systems are characterized by nonintegrable differential expressions, such as

$$\sum_{i=i}^{n} f_{ij}(q_1, q_2, \cdots, q_n, t)\dot{q}_i = 0, \;\; j = 1, 2, \cdots, m \tag{7.41}$$

where $\dot{q}_i$ represents the nth generalized coordinate (state variable), m is the number of equations defining the nonholonomic constraints, $\dot{q}_i$ represents the generalized speed and f_{ij} are nonlinear functions of q_i at time t. For the kinematic model of Eq. (7.40) the following nonholonomic constraint exists:

$$\dot{x}sin(\theta) - \dot{y}cos(\theta) = 0 \tag{7.42}$$

The curvature radius for any path can be written as

$$R(t) = \frac{1}{\rho(t)} = \frac{L}{tan(\phi)} \tag{7.43}$$

where L is the distance between the front and the back wheels, and ϕ (namely the steering angle) is the angle defined by the main axis of the vehicle and the velocity vector of the front wheel (for cart like vehicles as shown in Fig. 7.1, and for car-like vehicles as shown in Fig. 7.5). The value of $R(t)$ is usually bounded by R_{min}, the minimum curvature radius.

7.3.2.2 Controller Design for UGVs

Flatness-based control can be used for steering the vehicle along a desirable trajectory. In the case of the autonomous vehicle of Eq. (7.39) the flat output is the cartesian position of the center of the wheel axis, denoted as $\eta = (x, y)$, while the other model parameters can be written as:

$$v = \pm||\dot{\eta}|| \begin{pmatrix} cos(\theta) \\ sin(\theta) \end{pmatrix} = \frac{\dot{\eta}}{v} \; tan(\phi) = ldet(\dot{\eta}\ddot{\eta})/v^3 \tag{7.44}$$

where det stands for a matrix determinant. These formulas show simply that θ is the tangent angle of the curve and $tan(\phi)$ is the associated curvature. With

reference to a generic driftless nonlinear system $\dot{q},\ q \in R^n, w \in R^m$, dynamic feedback linearization consists in finding a feedback compensator of the form

$$\begin{aligned} \dot{\xi} &= \alpha(q,\xi) + b(q,\xi)u \\ w &= c(q,\xi) + d(q,\xi)u \end{aligned} \tag{7.45}$$

with state $\xi \in R^v$ and input $u \in R^m$, such that the closed-loop system of Eq. (7.39) and Eq. (7.45) is equivalent under a state transformation $z = T(q,\xi)$ to a linear system. The starting point is the selection of a m-dimensional output $\eta = h(q)$ to which a desired behavior can be assigned (this is the previously defined *flat output*). One then proceeds by successively differentiating the output until the input appears in a non-singular way. If the sum of the output differentiation orders equals the dimension $n + v$ of the extended state space, full input-state-output linearization is obtained. The closed-loop system is then equivalent to a set of decoupled input-output chains of integrators from u_i to η_i. The exact linearization procedure is illustrated for the vehicle's model of Eq. (7.39). As flat output $\eta = (x, y)$ the coordinates of the center of the wheel axis is considered. Differentiation with respect to time then yields [371, 439]

$$\dot{\eta} = \begin{pmatrix} \dot{x} \\ \dot{y} \end{pmatrix} = \begin{pmatrix} cos(\theta) & 0 \\ sin(\theta) & 0 \end{pmatrix} \cdot \begin{pmatrix} v \\ \omega \end{pmatrix} \tag{7.46}$$

showing that only v affects $\dot{\eta}$, while the angular velocity ω cannot be recovered from this first-order differential information. To proceed, one needs to add an integrator (whose state is denoted by ξ) on the linear velocity input

$$v = \xi,\ \dot{\xi} = \alpha \Rightarrow \dot{\eta} = \xi \begin{pmatrix} cos(\theta) \\ sin(\theta) \end{pmatrix} \tag{7.47}$$

where α denotes the linear acceleration of the vehicle. Differentiating further one obtains

$$\begin{aligned} \ddot{\eta} &= \dot{\xi} \begin{pmatrix} cos(\theta) \\ sin(\theta) \end{pmatrix} + \xi\dot{\theta} \begin{pmatrix} sin(\theta) \\ cos(\theta) \end{pmatrix} = \\ &= \begin{pmatrix} cos(\theta) & -\xi sin(\theta) \\ sin(\theta) & \xi cos(\theta) \end{pmatrix} \begin{pmatrix} \alpha \\ \omega \end{pmatrix} \end{aligned} \tag{7.48}$$

and the matrix multiplying the modified input (α, ω) is nonsingular if $\xi \neq 0$. Under this assumption one defines

$$\begin{pmatrix} \alpha \\ \omega \end{pmatrix} = \begin{pmatrix} cos(\theta) & -\xi sin(\theta) \\ sin(\theta) & \xi cos(\theta) \end{pmatrix} \cdot \begin{pmatrix} u_1 \\ u_2 \end{pmatrix} \tag{7.49}$$

and $\ddot{\eta}$ is denoted as

$$\ddot{\eta} = \begin{pmatrix} \ddot{\eta}_1 \\ \ddot{\eta}_2 \end{pmatrix} = \begin{pmatrix} u_1 \\ u_2 \end{pmatrix} = u \tag{7.50}$$

which means that the desirable linear acceleration and the desirable angular velocity can be expressed using the transformed control inputs u_1 and u_2. Then, the resulting dynamic compensator is (return to the initial control inputs v and ω)

$$\begin{aligned} \dot{\xi} &= u_1 cos(\theta) + u_2 sin(\theta) \\ v &= \xi \\ \omega &= \frac{u_2 cos(\theta) - u_1 sin(\theta)}{\xi} \end{aligned} \tag{7.51}$$

Being $\xi \in R$, it is $n + v = 3 + 1 = 4$, equal to the output differentiation order in Eq. (7.50). In the new coordinates

$$\begin{aligned} z_1 &= x \\ z_2 &= y \\ z_3 &= \dot{x} = \xi cos(\theta) \\ z_4 &= \dot{y} = \xi sin(\theta) \end{aligned} \tag{7.52}$$

The extended system is thus fully linearized and described by the chains of integrators, in Eq. (7.50), and can be rewritten as

$$\ddot{z}_1 = u_1, \quad \ddot{z}_2 = u_2 \tag{7.53}$$

The dynamic compensator of Eq. (7.51) has a potential singularity at $\xi = v = 0$, i.e. when the vehicle is not moving, which is a case not met while executing the trajectory tracking. It is noted however, that the occurrence of such a singularity is structural for non-holonomic systems. In general, this difficulty must be obviously taken into account when designing control laws on the equivalent linear model. A nonlinear controller for output trajectory tracking, based on dynamic feedback linearization, is easily derived. Assume that the autonomous vehicle must follow a smooth trajectory $(x_d(t), y_d(t))$ which is persistent, i.e. for which the nominal velocity $v_d = (\dot{x}_d^2 + \dot{y}_d^2)^{\frac{1}{2}}$ along the trajectory never goes to zeros (and thus singularities are avoided). On the equivalent and decoupled system of Eq. (7.53), one can easily design an exponentially stabilizing feedback for the desired trajectory, which has the form

$$\begin{aligned} u_1 &= \ddot{x}_d + k_{p_1}(x_d - x) + k_{d_1}(\dot{x}_d - \dot{x}) \\ u_2 &= \ddot{y}_d + k_{p_1}(y_d - y) + k_{d_1}(\dot{y}_d - \dot{y}) \end{aligned} \tag{7.54}$$

and which results in the following error dynamics for the closed-loop system

$$\begin{aligned} \ddot{e}_x + k_{d_1}\dot{e}_x + k_{p_1}e_x &= 0 \\ \ddot{e}_y + k_{d_2}\dot{e}_y + k_{p_2}e_y &= 0, \end{aligned} \tag{7.55}$$

where $e_x = x - x_d$ and $e_y = y - y_d$. The proportional-derivative gains are chosen as $k_{p_1} > 0$ and $k_{d_1} > 0$ for $i = 1, 2$. Knowing the control inputs u_1, u_2, for the linearized

system one can calculate the control inputs v and ω applied to the vehicle, using Eq. (7.45). The above result is valid, provided that the dynamic feedback compensator does not meet the singularity. In the general case of design of flatness-based controllers, the following theorem assures the avoidance of singularities in the proposed control law [371]:

Theorem: Let $\lambda_{11}, \lambda_{12}$ and $\lambda_{21}, \lambda_{22}$, be respectively the eigenvalues of two equations of the error dynamics, given in Eq. (7.45). Assume that, for $i = 1, 2$ it is $\lambda_{11} < \lambda_{12} < 0$ (negative real eigenvalues), and that λ_{i2} is sufficiently small. If

$$\min_{t \geq 0} || \begin{pmatrix} \dot{x}_d(t) \\ \dot{y}_d(t) \end{pmatrix} || \geq \begin{pmatrix} \dot{\epsilon}_x^0 \\ \dot{\epsilon}_y^0 \end{pmatrix} \tag{7.56}$$

with $\dot{\epsilon}_x^0 = \dot{\epsilon}_x(0) \neq 0$ and $\dot{\epsilon}_y^0 = \dot{\epsilon}_y(0) \neq 0$, then the singularity $\xi = 0$ is never met.

7.3.2.3 Derivative-Free Kalman Filtering for UGVs

It is assumed now that the vehicle's velocity has to be estimated through the processing of the sequence of position measurements by a filtering algorithm. To this end the derivative-free nonlinear Kalman Filter for MIMO nonlinear dynamical systems can been used. From the previous application of the differential flatness theory, it is possible to transform the initial nonlinear vehicle's model into a linearized equivalent model that is finally written in the Brunovsky form. Thus one arrives at Eq. (7.50) which means $\ddot{x} = u_1$ and $\ddot{y} = u_2$. Next, the state variables $x_1 = x$, $x_2 = \dot{x}$, $x_3 = y$ and $x_4 = \dot{y}$ are defined. Considering the state vector $x \in R^{4\times 1}$, the following matrices are also defined

$$A = \begin{pmatrix} 0 & 1 & 0 & 0 \\ 0 & 0 & 0 & 0 \\ 0 & 0 & 0 & 1 \\ 0 & 0 & 0 & 0 \end{pmatrix}, \quad B = \begin{pmatrix} 0 & 0 \\ 1 & 0 \\ 0 & 0 \\ 0 & 1 \end{pmatrix}, \quad C = \begin{pmatrix} 1 & 0 & 0 & 0 \\ 0 & 0 & 1 & 0 \end{pmatrix} \tag{7.57}$$

Using the matrices of Eq. (7.57) one obtains the Brunovsky form of the MIMO robot model

$$\begin{aligned} \dot{x} &= Ax + Bv \\ y &= Cx \end{aligned} \tag{7.58}$$

where the new input v is given by $v = [u_1(x, t), u_2(x, t)]^T$. For the unicycle robotic model of Eq. (7.58) state estimation can be performed using the standard Kalman Filter recursion, as described in Eqs. (4.88) and (4.89).

7.3.3 Simulation Tests

7.3.3.1 Extended Kalman Filter Based Navigation of the Autonomous Vehicle

The vehicle's kinematic model of Eq. (7.39) is considered. A GPS sensor or encoders placed at the vehicle's wheels can be used to provide measurements of the cartesian coordinates of the vehicle $x(t)$ and $y(t)$ (displacement of the vehicle), over a sampling period T. The values of the vehicle's velocity components along the x and y axes are not directly available and are estimated through the processing of the sequence of position measurements with the use of a filtering algorithm. Computing the vehicle's speed through the differentiation of the position measurements would introduce cumulative errors in the value of the vehicle's velocity, which in turn can affect the performance of the control loop. To avoid such errors an estimation of the vehicle's velocity is obtained through the processing of the sequence of position measurements with the use of a filtering algorithm.

Assuming a constant sampling period $\Delta t_k = T$ the measurement equation is $z(k+1) = \gamma(x(k)) + v(k)$, where $z(k)$ is the vector containing the sequence of measurements of the cartesian coordinates of the vehicle and $v(k)$ is the measurement noise vector.

$$z(k) = [x(k) + v_1(k), y(k) + v_2(k)], \ k = 1, 2, 3 \cdots \tag{7.59}$$

To obtain the Extended Kalman Filter (EKF), the kinematic model of the vehicle is linearized about the estimates $\hat{x}(k)$ and $\hat{x}^-(k)$, and the control input $U(k)$ is applied. Using that the continuous-time state-space description of the system is

$$\dot{x} = \phi(x, u) + wz = \gamma(x) + v \tag{7.60}$$

and by defining matrices $A = I + T_s J_x \phi(x, u)(x)$, $B = T_s J_u \phi(x, u)$ and $C = J_x \gamma(x)$ the linearized description of the system is obtained:

$$\begin{aligned} x(k+1) &= Ax + Bu(k) + w(k) \\ z(k) &= Cx(k) + v(k) \end{aligned} \tag{7.61}$$

The EKF recursion consists of the measurement update part and of the time update part as described in Eqs. (4.88) and (4.89), respectively.

One has to use the input gain matrix $B(k)$

$$B(k) = \begin{pmatrix} T_s cos(\theta(k)) & 0 \\ T_s sin(\theta(k)) & 0 \\ 0 & T \end{pmatrix} \tag{7.62}$$

and to compute the drift matrix $A(k)$ as follows

$$A(k) = \begin{pmatrix} 1 & 0 & -v(k)sin(\theta)T_s \\ 0 & 1 & v(k)cos(\theta)T_s \\ 0 & 0 & 1 \end{pmatrix} \tag{7.63}$$

while for the elements of the process noise covariance matrix which is given by $Q(k) = diag[\sigma^2(k), \sigma^2(k), \sigma^2(k)]$ indicative values would be $\sigma^2(k) = 10^{-3}$.

Using the estimated state vector, function $\phi(x)$ appearing in the state equations part and $\gamma(x)$ appearing in the measurements equations part of the vehicle's kinematic model become $\phi(\hat{x}(k)) = [\hat{x}(k), \hat{y}(k)]^T$, and $\gamma(\hat{x}(k)) = [\hat{x}(k), \hat{y}(k)]$, respectively. The associated Jacobian matrix $J_\gamma^T(\hat{x}^-(k))$ is given by

$$J_\gamma(\hat{x}^-(k)) = \begin{pmatrix} 1 & 0 & 0 \\ 0 & 1 & 0 \end{pmatrix} \tag{7.64}$$

The vehicle is steered by the flatness-based controller analyzed in Sect. 7.3.2

$$\begin{aligned} u_1 &= \ddot{x}_d + K_{p_1}(x_d - x) + K_{d_1}(\dot{x}_d - \dot{x}) \\ u_2 &= \ddot{y}_d + K_{p_2}(y_d - y) + K_{d_2}(\dot{y}_d - \dot{y}) \\ \dot{\xi} &= u_1 cos(\theta) + u_2 sin(\theta) \\ v = \xi, \;\; \omega &= \frac{u_2 cos(\theta) - u_1 sin(\theta)}{\xi} \end{aligned} \tag{7.65}$$

The use of EKF for estimating the vehicle's velocity along the x-axis (denoted as $\dot{x}$) and the vehicle's velocity along the y-axis (denoted as $\dot{y}$) enables the successful application of nonlinear steering control of Eq. (7.65).

Indicative results about tracking of the circular reference trajectory with use of the Extended Kalman Filter are shown in Figs. 7.6, 7.7, 7.8 and 7.9. In Fig. 7.6 one can notice the accuracy of tracking of the reference trajectory, achieved by the proposed state estimation-based control scheme. In Fig. 7.7 the accuracy of tracking of the x and y axis position setpoints is depicted. In Fig. 7.8, the associated x and y axis tracking errors are shown. Finally, in Fig. 7.9 the x and y axis velocity estimation errors are given.

Indicative results about tracking of the eight-shaped reference trajectory with use of the Extended Kalman Filter are shown in Figs. 7.10, 7.11 and 7.12 and 7.13. In Fig. 7.10 one can notice the accuracy of tracking of the reference trajectory, achieve by the proposed state estimation-based control scheme. In Fig. 7.11 the accuracy of tracking of the x and y axis position setpoints is depicted. In Fig. 7.12, the associated x and y axis tracking errors are shown. Finally, in Fig. 7.13 the x and y axis velocity estimation errors are given.

Indicative results about tracking of the complex-curved reference trajectory with use of the Extended Kalman Filter are shown in Figs. 7.14, 7.15, 7.16 and 7.17. In Fig. 7.14 one can notice the accuracy of tracking of the reference trajectory, achieve by the proposed state estimation-based control scheme. In Fig. 7.15 the accuracy of

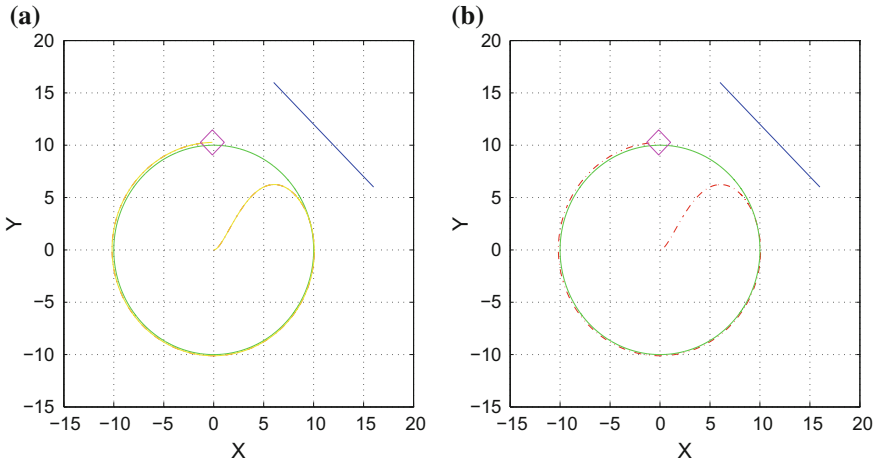

Fig. 7.6 **a** Tracking of a circular reference trajectory (green line) by the autonomous vehicle and associated estimation of the vehicle's position provided by the Extended Kalman Filter (continuous yellow line) **b** Tracking of a circular reference trajectory (green line) by the autonomous vehicle and real position of the vehicle (dashed red line)

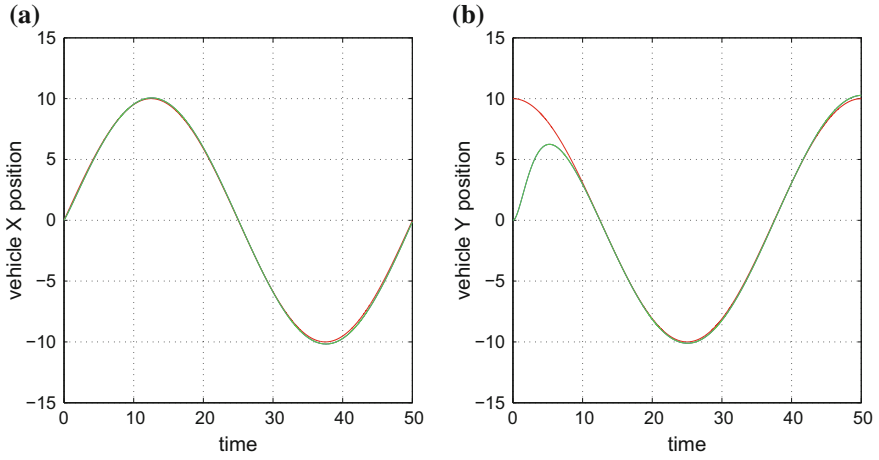

Fig. 7.7 Tracking of a circular reference trajectory with use of the EKF: **a** tracking of the x-axis reference set-point **b** tracking of the y-axis reference set-point

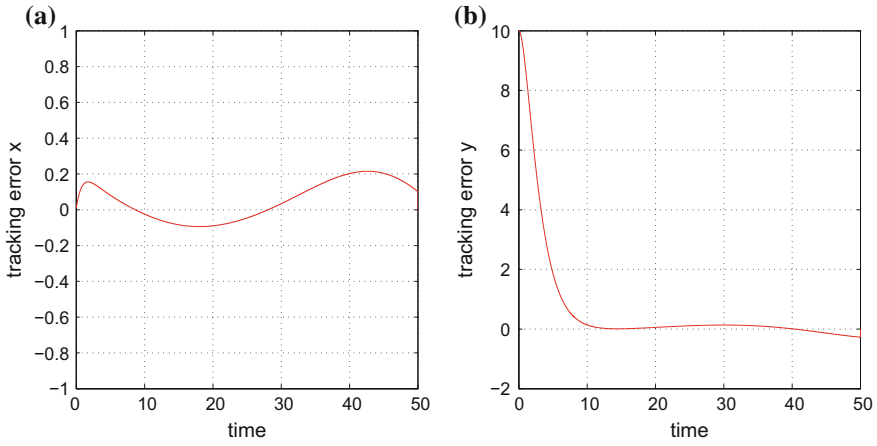

Fig. 7.8 Tracking of a circular reference trajectory with use of the EKF: **a** tracking error along the x-axis **b** tracking error along the y-axis

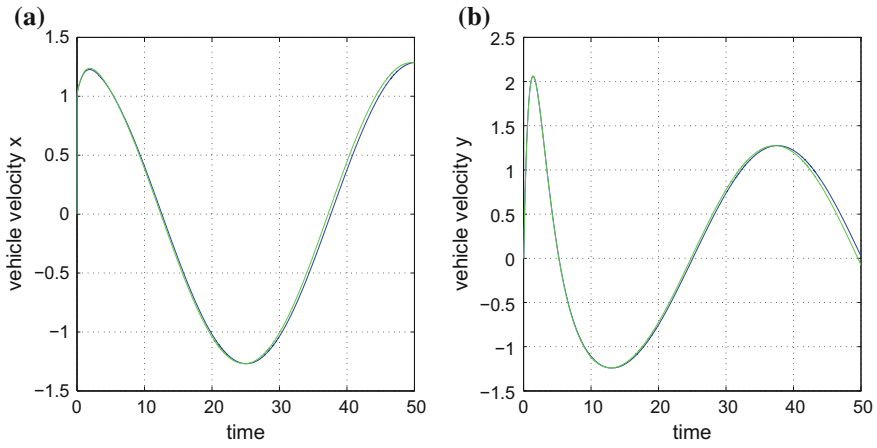

Fig. 7.9 Tracking of a circular reference trajectory by the autonomous vehicle with use of the EKF: **a** convergence of the estimated x-axis velocity (green line) to the associated real velocity (blue line) **b** convergence of the estimated y-axis velocity (green line) to the associated real velocity (green line)

tracking of the x and y axis position setpoints is depicted. In Fig. 7.16, the associated x and y axis tracking errors are shown. Finally, in Fig. 7.17 the x and y axis velocity estimation errors are given.

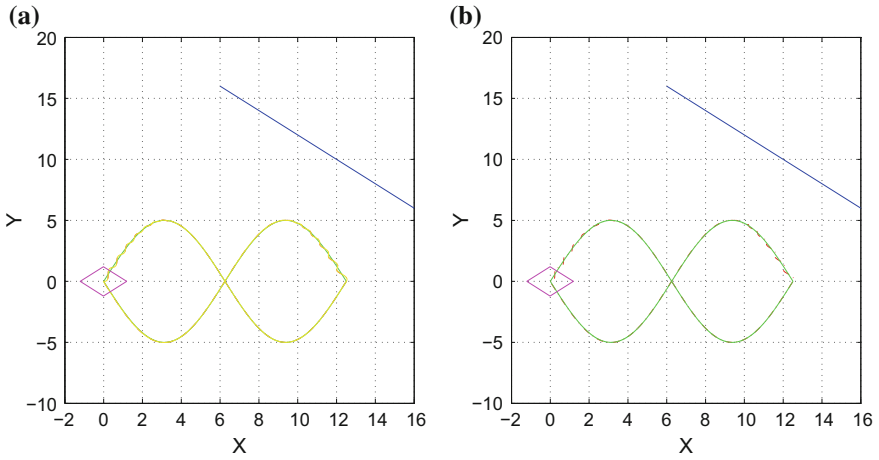

Fig. 7.10 **a** Tracking of an eight-shaped reference trajectory (green line) by the autonomous vehicle and associated estimation of the vehicle's position provided by the Extended Kalman Filter (yellow line) **b** Tracking of a circular reference trajectory (green line) by the autonomous vehicle and real position of the vehicle (dashed red line)

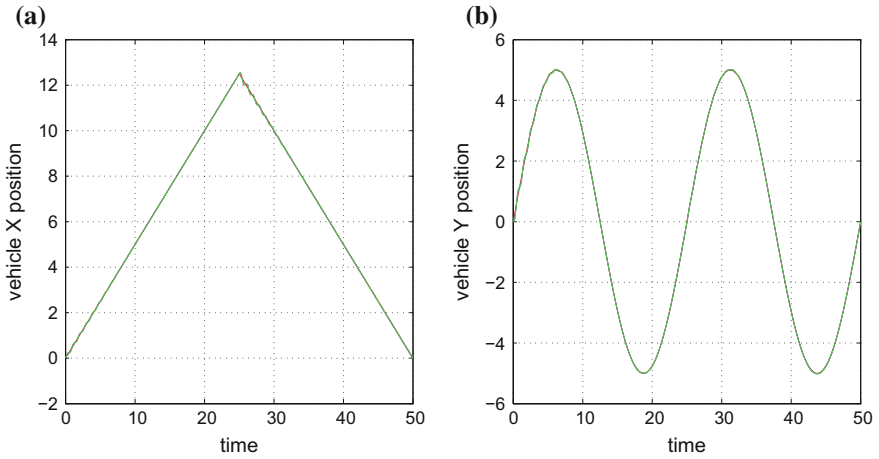

Fig. 7.11 Tracking of an eight-shaped reference trajectory with use of the EKF: **a** tracking of the x-axis reference set-point **b** tracking of the y-axis reference set-point

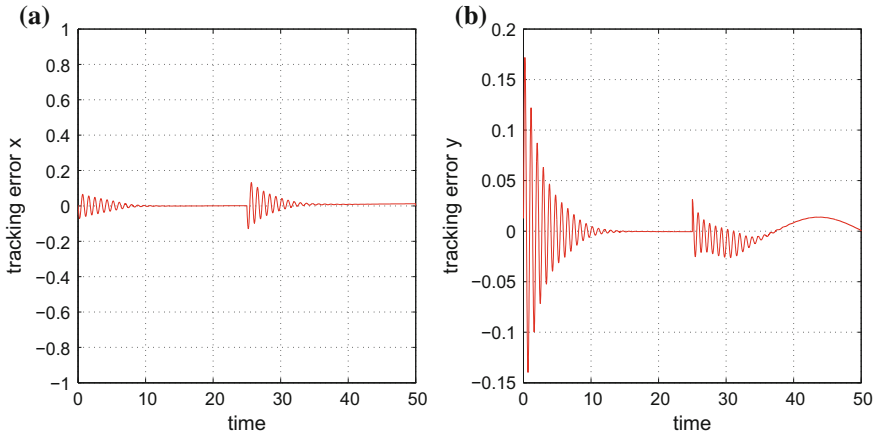

Fig. 7.12 Tracking of an eight-shaped reference trajectory with use of the EKF: **a** tracking error along the x-axis **b** tracking error along the y-axis

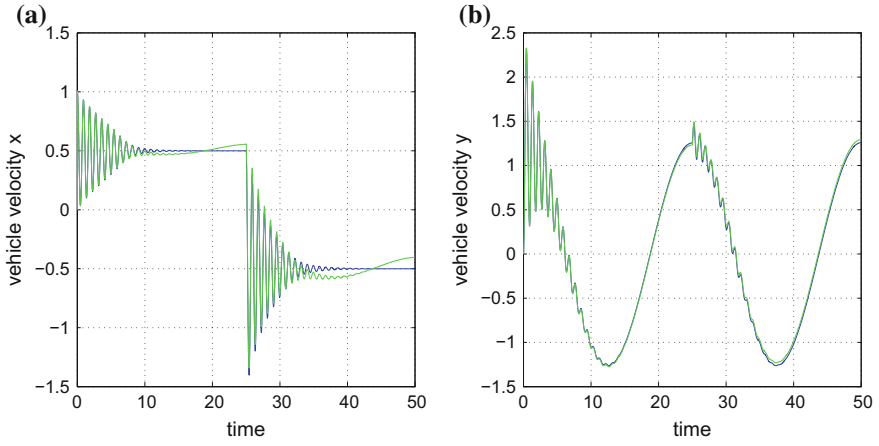

Fig. 7.13 Tracking of an eight-shaped reference trajectory by the autonomous vehicle with use of the EKF: **a** convergence of the estimated x-axis velocity (green line) to the associated real velocity (blue line) **b** convergence of the estimated y-axis velocity (green line) to the associated real velocity (green line)

7.3.3.2 Derivative-Free Kalman Filter Based Navigation of the Autonomous Vehicle

A second set of tests focused on the performance of the proposed Derivative-free nonlinear Kalman Filter (DKF) in the problem of state estimation-based control of an autonomous vehicle (cart-like robot) (Fig. 7.1). The differentially flat model of the autonomous vehicle and its transformation to the Brunovksy form has been

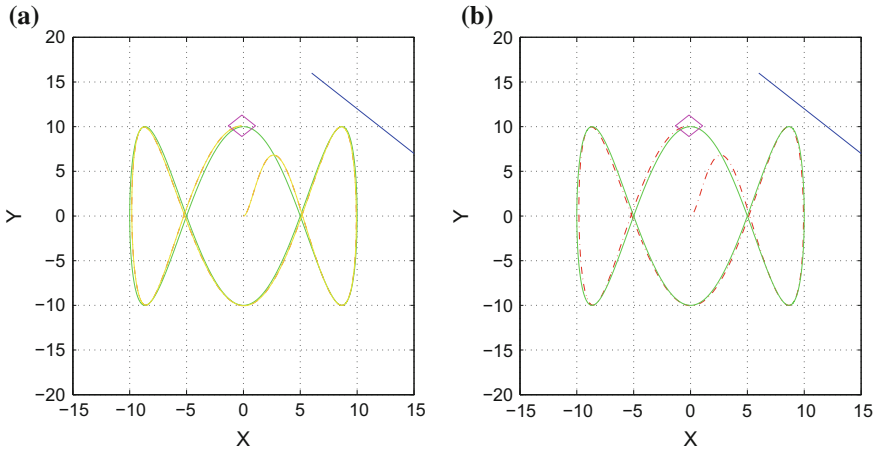

Fig. 7.14 **a** Tracking of a complex-curved reference trajectory (green line) by the autonomous vehicle and associated estimation of the vehicle's position provided by the Extended Kalman Filter (yellow line) **b** Tracking of a circular reference trajectory (green line) by the autonomous vehicle (red dashed line) and real position of the vehicle (dashed red line)

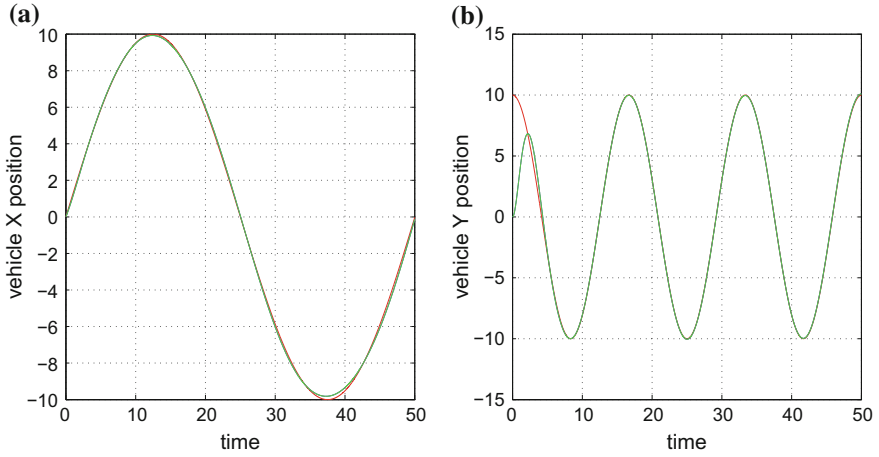

Fig. 7.15 Tracking of a complex-curved reference trajectory with use of the EKF: **a** tracking of the x-axis reference set-point **b** tracking of the y-axis reference set-point

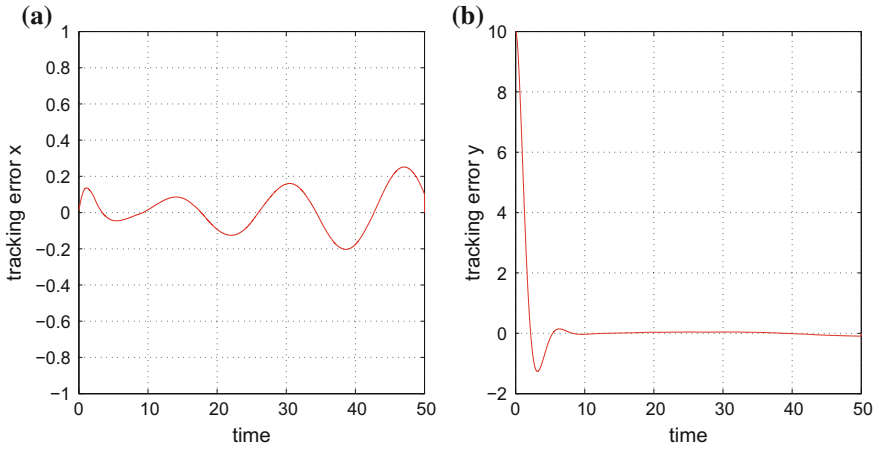

Fig. 7.16 Tracking of a complex-curved reference trajectory with use of the EKF: **a** tracking error along the x-axis **b** tracking error along the y-axis

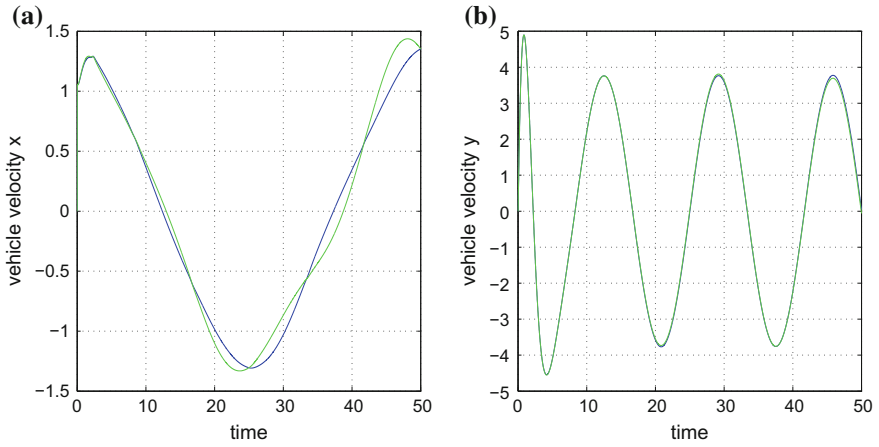

Fig. 7.17 Tracking of a complex-curved reference trajectory by the autonomous vehicle with use of the EKF: **a** convergence of the estimated x-axis velocity (green line) to the associated real velocity (blue line) **b** convergence of the estimated y-axis velocity (green line) to the associated real velocity (green line)

analyzed in Eqs. (7.39) and (7.46). The state estimation algorithm of the Derivative-free nonlinear Kalman Filter consisted of Eqs. (4.88) and (4.89). It was assumed that only measurements of the cartesian coordinates of the vehicle (displacement on the xy-plane) could be obtained through a GPS unit (localization of moderate accuracy), RTK-GPS (localization of higher accuracy) or through laser, visual and sonar sensors with reference to specific landmarks (the latter measuring approaches require transformation from a local to a global coordinates system).

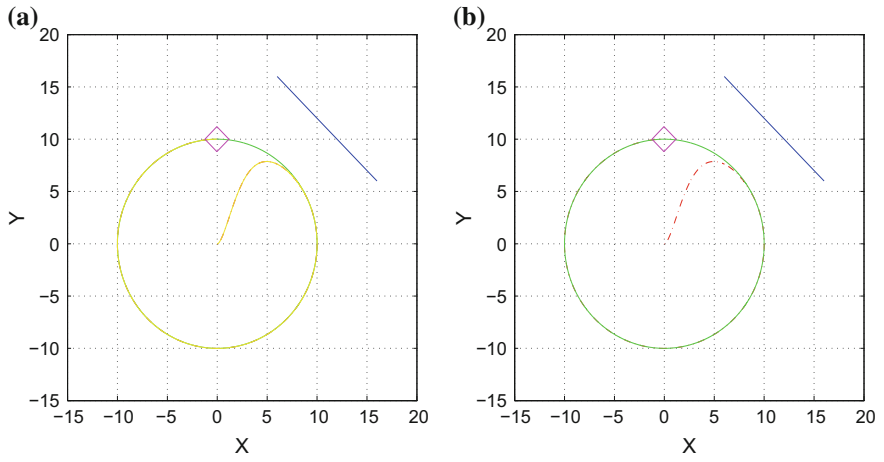

Fig. 7.18 **a** Tracking of a circular reference trajectory (green line) by the autonomous vehicle and associated estimation of the vehicle's position provided by the derivative-free Kalman Filter (yellow line) **b** Tracking of a circular reference trajectory (green line) by the autonomous vehicle and real position of the vehicle (dashed red line)

Indicative results about tracking of the circular reference trajectory with use of the Derivative-free nonlinear Kalman Filter are shown in Figs. 7.18, 7.19 and 7.20. Comparing the estimation performed by the derivative-free MIMO nonlinear Kalman Filter with the one performed by the Extended Kalman Filter it can be noticed that the derivative-free filtering approach results in more accurate state estimates.

Indicative results about tracking of the circular reference trajectory with use of the Derivative-free nonlinear Kalman Filter are shown in Figs. 7.18, 7.19 and 7.20. In Fig. 7.18 one can notice the accuracy of tracking of the reference trajectory, achieved by the proposed state estimation-based control scheme. In Fig. 7.19, the associated x and y axis tracking errors are shown. Finally, in Fig. 7.20 the x and y axis velocity estimation errors are given.

Indicative results about tracking of the eight-shaped reference trajectory with use of the Extended Kalman Filter are shown in Figs. 7.21, 7.22, 7.23 and 7.24. In Fig. 7.21 one can notice the accuracy of tracking of the reference trajectory, achieved by the proposed state estimation-based control scheme. In Fig. 7.22 the accuracy of tracking of the x and y axis position setpoints is depicted. In Fig. 7.23, the associated x and y axis tracking errors are shown. Finally, in Fig. 7.24 the x and y axis velocity estimation errors are given.

Indicative results about tracking of the complex-curved reference trajectory with use of the Extended Kalman Filter are shown in Figs. 7.25, 7.26, 7.27 and 7.28. In Fig. 7.25 one can notice the accuracy of tracking of the reference trajectory, achieved by the proposed state estimation-based control scheme. In Fig. 7.26 the accuracy of tracking of the x and y axis position setpoints is depicted. In Fig. 7.27, the associated

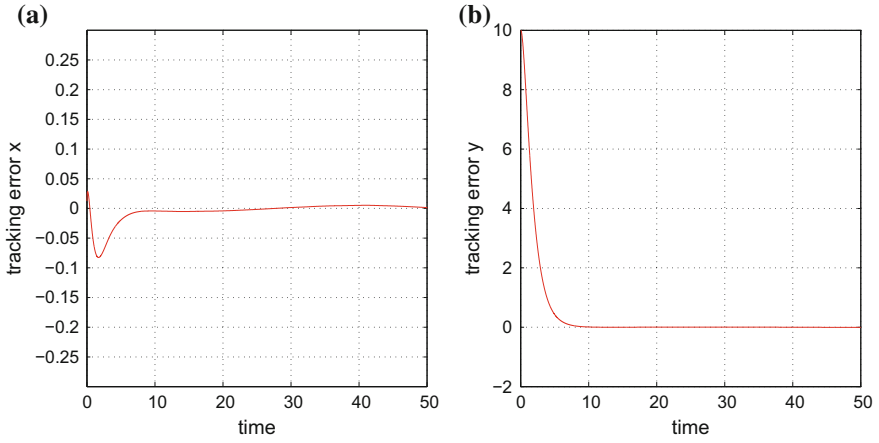

Fig. 7.19 Tracking of a circular reference trajectory with use if the DKF: **a** tracking error along the x-axis **b** tracking error along the y-axis

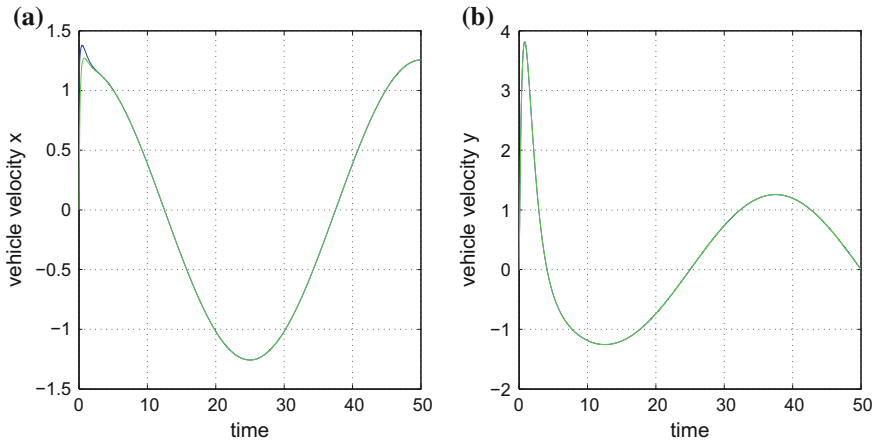

Fig. 7.20 Tracking of a circular reference trajectory by the autonomous vehicle with use of the DKF: **a** convergence of the estimated x-axis velocity (green line) to the associated real velocity (blue line) **b** convergence of the estimated y-axis velocity (green line) to the associated real velocity (green line)

x and y axis tracking errors are shown. Finally, in Fig. 7.28 the x and y axis velocity estimation errors are given.

Comparing the estimation performed by the Derivative-free nonlinear Kalman Filter with the one performed by the Extended Kalman Filter it can be noticed that the derivative-free filtering approach results in more accurate state estimates. Moreover, comparing the associated state estimation-based control loop of the autonomous vehicle that was based on the derivative-free MIMO nonlinear Kalman Filter to the

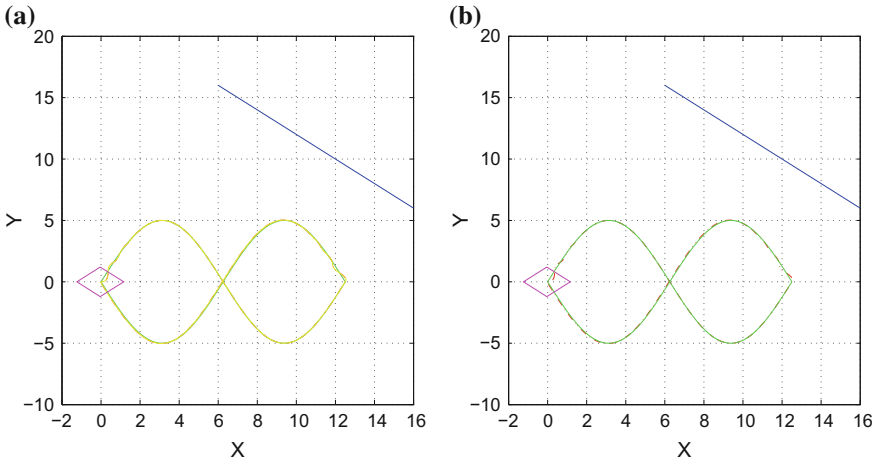

Fig. 7.21 **a** Tracking of an eight-shaped reference trajectory (green line) by the autonomous vehicle and associated estimation of the vehicle's position provided by the derivative-free Kalman Filter (yellow line) **b** Tracking of a circular reference trajectory (green line) by the autonomous vehicle and real position of the vehicle (dashed red line)

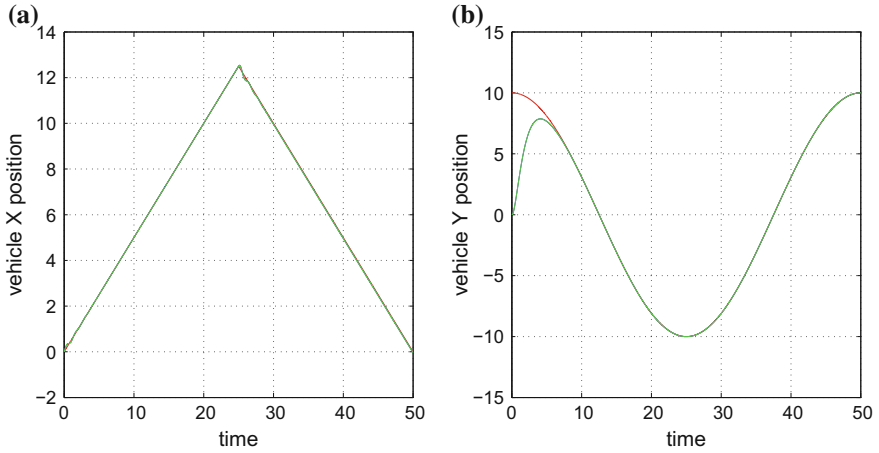

Fig. 7.22 Tracking of an eight-shaped reference trajectory with use of the DKF: **a** tracking of the x-axis reference set-point **b** tracking of the y-axis reference set-point

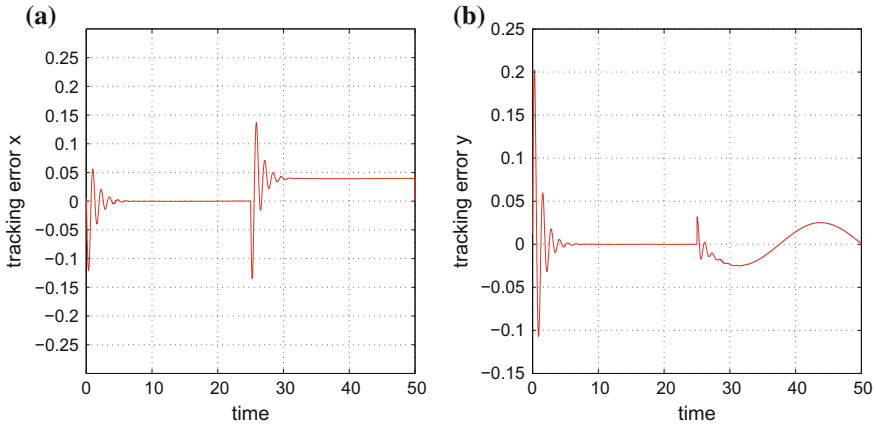

Fig. 7.23 Tracking of an eight-shaped reference trajectory with use of the DKF: **a** tracking error along the x-axis **b** tracking error along the y-axis

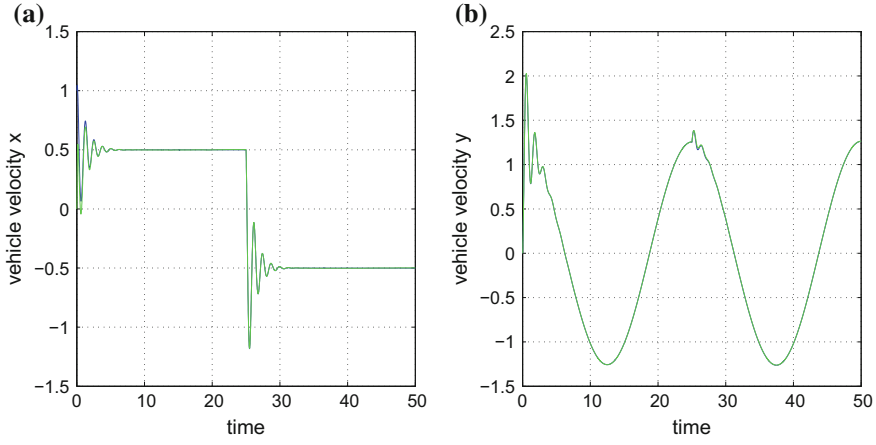

Fig. 7.24 Tracking of an eight-shaped reference trajectory by the autonomous vehicle with use of the DKF: **a** convergence of the estimated x-axis velocity (green line) to the associated real velocity (blue line) **b** convergence of the estimated y-axis velocity (green line) to the associated real velocity (green line)

control that relied on the Extended Kalman Filter it was observed that the first control scheme was significantly more robust and capable of tracking with better accuracy the desirable trajectories. These findings show the suitability of the considered Derivative-free nonlinear Kalman Filter for localization, control and autonomous navigation of autonomous vehicles. Finally, it is noted that the section's approach can be applied also to various types of 4-wheel robotic vehicles.

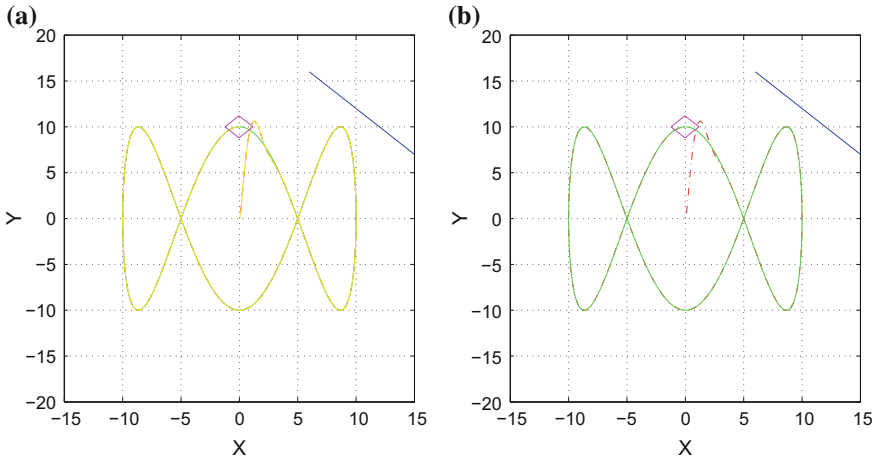

Fig. 7.25 **a** Tracking of a complex-curved reference trajectory (green line) by the autonomous vehicle and associated estimation of the vehicle's position provided by the derivative-free Kalman Filter (yellow line) **b** Tracking of a circular reference trajectory (green line) by the autonomous vehicle and real position of the vehicle (dashed red line)

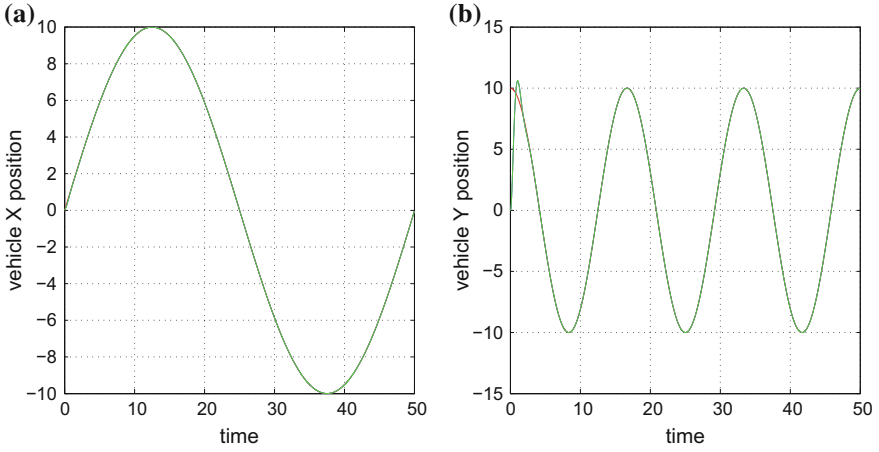

Fig. 7.26 Tracking of a complex-curved reference trajectory with use of the DKF: **a** tracking of the x-axis reference set-point **b** tracking of the y-axis reference set-point

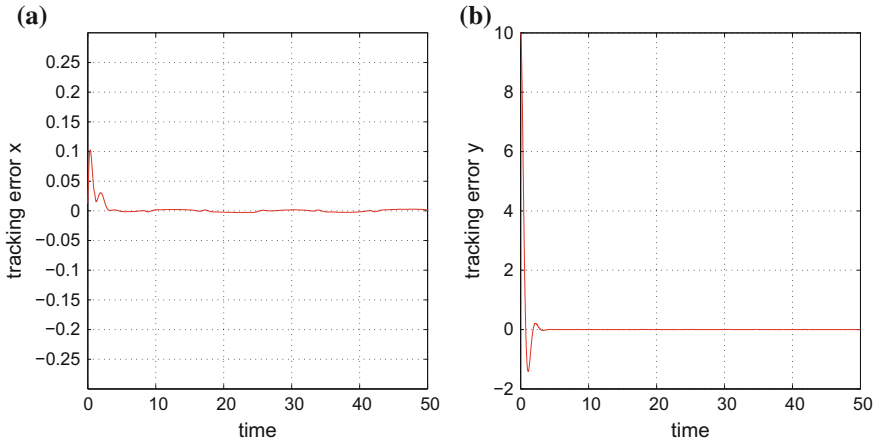

Fig. 7.27 Tracking of a complex-curved reference trajectory with use of the DKF: **a** tracking error along the x-axis **b** tracking error along the y-axis

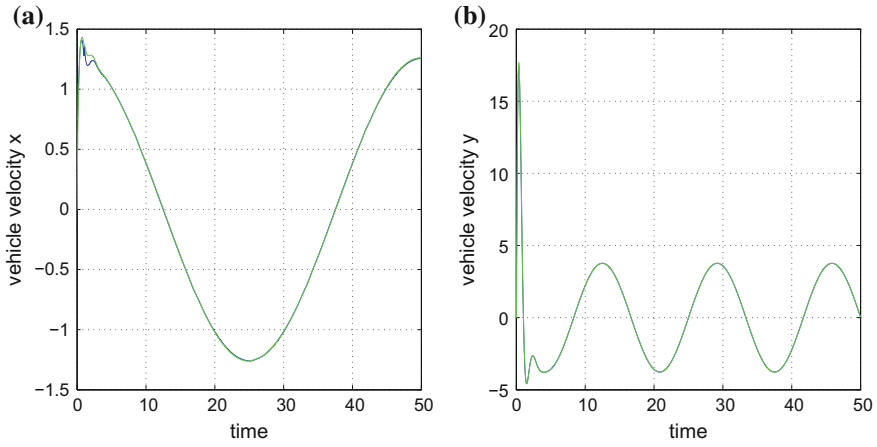

Fig. 7.28 Tracking of a complex-curved reference trajectory by the autonomous vehicle with use of the DKF: **a** convergence of the estimated x-axis velocity (green line) to the associated real velocity (blue line) **b** convergence of the estimated y-axis velocity (green line) to the associated real velocity (green line)

7.4 Nonlinear Optimal Control of Autonomous Two-Wheel Vehicles

7.4.1 Outline

Autonomous or semi-autonomous navigation of two-wheel vehicles such as motorcycles, requires that several of their functionalities and driving tasks, are automatically performed [74, 81, 154, 615, 626]. To achieve this objective, the need of developing and using elaborated control and estimation methods for motorcycles has become apparent [15, 324, 479, 481, 610]. To this end, several results have been developed aiming at solving the stabilization and path tracking problems for autonomous or semi-autonomous motorcycles [71, 104, 114, 173, 293, 410, 565]. Due to underactuation in the motorcycle's model and the strong nonlinearities characterizing its state-space description, the solution of the associated motion problem is a difficult and challenging endeavour [102, 103, 113, 115]. To achieve a satisfactory solution of the problem of autonomous motorcycles driving, in this section a nonlinear optimal (H-infinity) controller is developed [419, 461].

First, the joint kinematic and dynamic model of the motorcycle undergoes approximate linearization around a temporary operating point (equilibrium) which is recomputed at each iteration of the control method. This equilibrium is defined by the present value of the system's state vector and the last value of the control inputs vector that was exerted on it. The linearization procedure requires first order Taylor series expansion of the state-space description of the motorcycle and computation of the associated Jacobian matrices [33, 431, 463]. The modelling error which is due to the truncation of higher-order terms in the Taylor series expansion is considered to be a disturbance which is eliminated by the robustness of the control loop. Next, for the approximately linearized model of the motorcycle an optimal (H-infinity) feedback controller is designed.

The H-infinity controller represents the solution of the optimal control problem for the model of the autonomous motorcycle, under model uncertainty and external perturbations. It actually stands for the solution of a min-max differential game, in which the controller tries to minimize a cost function comprising a quadratic term of the state vector's tracking error, whereas the model uncertainty and external perturbation terms try to maximize this cost function. For the computation of the controller's feedback gain it is necessary to solve an algebraic Riccati equation at each time-step of the control method [450, 457, 459]. The stability properties of the control method are proven through Lyapunov analysis. First, it is demonstrated that the control loop of the motorcycle satisfies the H-infinity tracking performance criterion. This signifies elevated robustness against model uncertainty and external perturbations affecting the motorcycle's motion [305, 564]. Next, it is proven that the control loop is also globally asymptotically stable, which ascertains precise tracking of reference paths. Moreover, to implement a state estimation-based control scheme for the autonomous motorcycle, through the processing of measurements from a small number of on-board sensors, the H-infinity Kalman Filter is proposed as a robust state estimator [169, 511].

7.4.2 Dynamic and Kinematic Model of the Riderless Motorcycle

As noted above the control and stabilization problem of the autonomous motorcycle is a nontrivial one. The use of nonlinear optimal (H-infinity) control for this problem is in several aspects advantageous. Comparing for instance against global linearization-based control schemes, the proposed nonlinear optimal control does not require complicated transformations (diffeomorphisms) for bringing the state-space model of the system into an equivalent linear form. Besides, it does not come against singularity problems because for computing the control inputs that will be finally exerted on the vehicle's model there is no need to implement inverse transformations which in-turn imply matrices inversions. Comparing against other optimal control methods it can be noted that Model Predictive Control is unsuitable for the model of the autonomous motorcycle because such a control method is addressed to linear dynamical systems and cannot compensate for strong nonlinearities. It can be also noted that Nonlinear Model Predictive Control, being a popular optimal control approach for nonlinear dynamical systems is not of assured convergence while its iterative search for an optimum is dependent on initial parametrization. On the other side, backstepping control cannot be directly applied to the model of the of the autonomous motorcycle because this is not inherently found in the triangular form. Furthermore, the application of sliding-mode control is hindered by the fact that the model of the autonomous motorcycle is not found inherently into a canonical form. Finally, PID control which is widely used by practitioners in the area of robotics is an unreliable methodology because the tuning of such a controller is performed in a heuristic manner around local operating points where the unrealistic assumption is made that the dynamics of the autonomous motorcycle remains linear. Such a control method lacks a global stability proof.

The main parameters of the autonomous motorcycle are described in Fig. 7.29. By defining as $\sigma = \frac{tan(\delta)}{p}$ the joint kinematic and dynamic model of the riderless motorcycle is given by [154]

$$\dot{x} = vcos(\psi) \tag{7.66}$$

$$\dot{y} = vsin(\psi) \tag{7.67}$$

$$\dot{\psi} = v\frac{tan(\delta)}{p} \tag{7.68}$$

$$\ddot{\phi} = \frac{1}{h}\{gsin(\phi) + cos(\psi)[(1 + h\sigma sin(\phi))\sigma v^2 + h\ddot{\psi}]\} \tag{7.69}$$

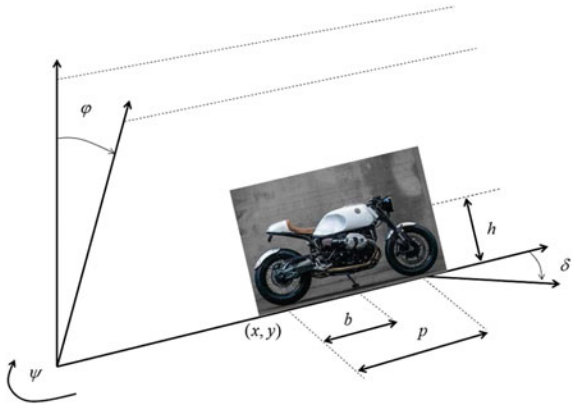

Fig. 7.29 Diagram of the two-wheel autonomous vehicle (riderless motorcycle)

By differentiating Eq. (7.68) one obtains [154]:

$$\ddot{\psi} = v\frac{\dot{\delta}}{pcos^2(\delta)} + \dot{v}\frac{\tan(\delta)}{p} \tag{7.70}$$

The following state variables are defined: $x_1 = x$, $x_2 = y$, $x_3 = \psi$, $x_4 = \phi$, $x_5 = \dot{\phi}$, $x_6 = v$, $x_7 = \delta$. Moreover, the following control inputs are defined $u_1 = \dot{v}$, $u_2 = \dot{\delta}$, that is the control inputs of the autonomous motorcycle are its acceleration and the rate of turn of the angle of its steering wheel. The state-space description of the system becomes:

$$\begin{gathered}
\dot{x}_1 = x_6 cos(x_3) \\
\dot{x}_2 = x_6 sin(x_3) \\
\dot{x}_3 = x_6\frac{tan(x_7)}{p} \\
\dot{x}_4 = x_5 \\
\dot{x}_5 = \frac{1}{h}\left\{gsin(x_4) + cos(x_4)\left[(1 + h\sigma sin(x_4))\sigma x_6^2 + bcos(x_4)\left(u_2\frac{x_6}{pcos^2(x_7)} + u_1\frac{tan(x_7)}{p}\right)\right]\right\} \\
\dot{x}_6 = u_1 \\
\dot{x}_7 = u_2
\end{gathered} \tag{7.71}$$

In vector form, one obtains the state-space description

$$\dot{x} = f(x) + G(x)u \tag{7.72}$$

where $G(x) = [g_1(x)\ g_2(x)]$ is the control inputs gain, or analytically

$$\begin{pmatrix}\dot{x}_1\\ \dot{x}_2\\ \dot{x}_3\\ \dot{x}_4\\ \dot{x}_5\\ \dot{x}_6\\ \dot{x}_7\end{pmatrix} = \begin{pmatrix} x_6 cos(x_3)\\ x_6 sin(x_3)\\ x_6 \frac{tan(x_7)}{p}\\ x_5\\ \frac{1}{h}\{g sin(x_4 + cos(x_4)[(1 + h\sigma sin(x_4))\sigma x_6^2])\}\\ 0\\ 0\end{pmatrix} + \\ + \begin{pmatrix} 0 & 0\\ 0 & 0\\ 0 & 0\\ 0 & 0\\ \frac{bcos(x_4)tan(x_7)}{p} & \frac{bcos(x_4)x_6}{pcos^2(x_7)}\\ 1 & 0\\ 0 & 1\end{pmatrix}\begin{pmatrix}u_1\\ u_2\end{pmatrix} \tag{7.73}$$

7.4.3 Approximate Linearization of the Model of the Riderless Motorcycle

Linearization is performed around the temporary operating point (x^*, u^*), where x^* is the present value of the state-vector of the two-wheel unmanned vehicle and u^* is the last value of the control input vector that was exerted on it. One has the linearized model $\dot{x} = Ax + Bu + \tilde{d}$ with:

$$A = \nabla_x[f(x) + G(x)u] \mid_{(x^*,u^*)} \Rightarrow \\ A = [\nabla_x f(x) + \nabla_x g_1(x)u_1 + \nabla_x g_2(x)u_2] \mid_{(x^*,u^*)} \tag{7.74}$$

$$B = \nabla_u[f(x) + G(x)u] \mid_{(x^*,u^*)} \Rightarrow \\ B = G(x) \mid_{(x^*,u^*)} \tag{7.75}$$

About the Jacobian matrix $\nabla_x f(x)|_{(x^*,u^*)}$ one has

$$\nabla_x f(x) \mid_{(x^*,u^*)} = \begin{pmatrix} \frac{\partial f_1}{\partial x_1} & \frac{\partial f_1}{\partial x_2} & \dots & \frac{\partial f_1}{\partial x_7}\\ \frac{\partial f_2}{\partial x_1} & \frac{\partial f_2}{\partial x_2} & \dots & \frac{\partial f_2}{\partial x_7}\\ \dots & \dots & \dots & \dots\\ \frac{\partial f_7}{\partial x_1} & \frac{\partial f_7}{\partial x_2} & \dots & \frac{\partial f_7}{\partial x_7}\end{pmatrix} \mid_{(x^*,u^*)} \tag{7.76}$$

For the first row of the Jacobian matrix $\nabla_x f(x)|_{(x^*,u^*)}$ it holds: $\frac{\partial f_1}{\partial x_1} = 0$, $\frac{\partial f_1}{\partial x_2} = 0$, $\frac{\partial f_1}{\partial x_3} = -x_6 sin(x_3)$, $\frac{\partial f_1}{\partial x_4} = 0$, $\frac{\partial f_1}{\partial x_5} = 0$, $\frac{\partial f_1}{\partial x_6} = cos(x_3)$, $\frac{\partial f_1}{\partial x_7} = 0$.

For the second row of the Jacobian matrix $\nabla_x f(x)|_{(x^*,u^*)}$ it holds: $\frac{\partial f_2}{\partial x_1} = 0$, $\frac{\partial f_2}{\partial x_2} = 0$, $\frac{\partial f_2}{\partial x_3} = x_6 cos(x_3)$, $\frac{\partial f_2}{\partial x_4} = 0$, $\frac{\partial f_2}{\partial x_5} = 0$, $\frac{\partial f_2}{\partial x_6} = 0 sin(x_3)$, $\frac{\partial f_1}{\partial x_7} = 0$.

For the third row of the Jacobian matrix $\nabla_x f(x)|_{(x^*,u^*)}$ it holds: $\frac{\partial f_3}{\partial x_1} = 0$, $\frac{\partial f_3}{\partial x_2} = 0$, $\frac{\partial f_3}{\partial x_3} = 0$, $\frac{\partial f_3}{\partial x_4} = 0$, $\frac{\partial f_3}{\partial x_5} = 0$, $\frac{\partial f_3}{\partial x_6} = \frac{tan(x_7)}{p}$, $\frac{\partial f_3}{\partial x_7} = x_6 \frac{1}{pcos^2(x_7)}$.

For the fourth row of the Jacobian matrix $\nabla_x f(x)|_{(x^*,u^*)}$ it holds: $\frac{\partial f_4}{\partial x_1} = 0$, $\frac{\partial f_4}{\partial x_2} = 0$, $\frac{\partial f_4}{\partial x_3} = 0$, $\frac{\partial f_4}{\partial x_4} = 0$, $\frac{\partial f_4}{\partial x_5} = 1$, $\frac{\partial f_4}{\partial x_6} = 0$, $\frac{\partial f_4}{\partial x_7} = 0$.

For the Jacobian's $\nabla_x f(x)|_{(x^*,u^*)}$ fifth row it holds: $\frac{\partial f_5}{\partial x_1} = 0$, $\frac{\partial f_5}{\partial x_2} = 0$, $\frac{\partial f_5}{\partial x_3} = 0$, $\frac{\partial f_5}{\partial x_4} = \frac{1}{h}\{gcos(x_4) - sin(x_4)[(1 + h\frac{tan(x_7)}{p}sin(x_4))\frac{tan(x_7)}{p}x_6^2] + cos(x_4)[h\frac{tan(x_7)}{p}cos(x_4)\frac{tan(x_7)}{p}x_6^2]\}$, $\frac{\partial f_5}{\partial x_5} = 0$, $\frac{\partial f_5}{\partial x_6} = \frac{1}{h}cos(x_4)[1 + h\frac{tan(x_7)}{p}sin(x_4))\frac{tan(x_7)}{p}2x_6]$, and continuing in a similar manner $\frac{\partial f_5}{\partial x_7} = \frac{1}{h}cos(x_4)\{[(h\frac{1}{pcos^2(x_7)}sin(x_4))\frac{tan(x_7)}{p}x_6^2] + [(1 + h\frac{tan(x_7)}{p}sin(x_4))\frac{1}{pcos^2(x_7)}x_6^2]\}$.

For the sixth row of the Jacobian matrix $\nabla_x f(x)|_{(x^*,u^*)}$ it holds: $\frac{\partial f_6}{\partial x_1} = 0$, $\frac{\partial f_6}{\partial x_2} = 0$, $\frac{\partial f_6}{\partial x_3} = 0$, $\frac{\partial f_6}{\partial x_4} = 0$, $\frac{\partial f_6}{\partial x_5} = 0$, $\frac{\partial f_6}{\partial x_6} = 0$, $\frac{\partial f_6}{\partial x_7} = 0$.

For the seventh row of the Jacobian matrix $\nabla_x f(x)|_{(x^*,u^*)}$ it holds: $\frac{\partial f_7}{\partial x_1} = 0$, $\frac{\partial f_7}{\partial x_2} = 0$, $\frac{\partial f_7}{\partial x_3} = 0$, $\frac{\partial f_7}{\partial x_4} = 0$, $\frac{\partial f_7}{\partial x_5} = 0$, $\frac{\partial f_7}{\partial x_6} = 0$, $\frac{\partial f_7}{\partial x_7} = 0$.

About the Jacobian matrix $\nabla_x g_1(x)|_{(x^*,u^*)}$ one has

$$\nabla_x g_1(x)\,|_{(x^*,u^*)} = \begin{pmatrix} 0\,0\,0 & 0 & 0\,0 & 0 \\ 0\,0\,0 & 0 & 0\,0 & 0 \\ 0\,0\,0 & 0 & 0\,0 & 0 \\ 0\,0\,0 & 0 & 0\,0 & 0 \\ 0\,0\,0 & bsin(x_4)\frac{tan(x_7)}{p} & 0\,0 & bcos(x_4)\frac{1}{pcos^2(x_7)} \\ 0\,0\,0 & 0 & 0\,0 & 0 \\ 0\,0\,0 & 0 & 0\,0 & 0 \end{pmatrix} |_{(x^*,u^*)} \tag{7.77}$$

About the Jacobian matrix $\nabla_x g_2(x)|_{(x^*,u^*)}$ one has

$$\nabla_x g_2(x)\,|_{(x^*,u^*)} = \begin{pmatrix} 0\,0\,0 & 0 & 0 & 0 & 0 \\ 0\,0\,0 & 0 & 0 & 0 & 0 \\ 0\,0\,0 & 0 & 0 & 0 & 0 \\ 0\,0\,0 & 0 & 0 & 0 & 0 \\ 0\,0\,0 & -\frac{bsin(x_4)x_6}{pcos^2(x_7)} & 0 & \frac{bcos(x_4)}{pcos^2(x_7)} & \frac{bcos(x_4)x_6sin(x_7)}{pcos^3(x_7)} \\ 0\,0\,0 & 0 & 0 & 0 & 0 \\ 0\,0\,0 & 0 & 0 & 0 & 0 \end{pmatrix} |_{(x^*,u^*)} \tag{7.78}$$

7.4.4 The Nonlinear H-Infinity Control

7.4.4.1 Tracking Error Dynamics for the Autonomous Motorcycle

The initial nonlinear model of the autonomous motorcycle is in the form

$$\dot{x} = f(x, u) \;\; x \in R^n, \;\; u \in R^m \tag{7.79}$$

Linearization of the model of the riderless motorcycle is performed at each iteration of the control algorithm round its present operating point $(x^*, u^*) = (x(t), u(t - T_s))$. The linearized equivalent of the autonomous motorcycle is described by

$$\dot{x} = Ax + Bu + L\tilde{d} \;\; x \in R^n, \;\; u \in R^m, \;\; \tilde{d} \in R^q \tag{7.80}$$

Thus, after linearization round its current operating point, the motorcycle's dynamic model is written as

$$\dot{x} = Ax + Bu + d_1 \tag{7.81}$$

Parameter d_1 stands for the linearization error in the two-wheel vehicle's dynamic model appearing in Eq. (7.81). The reference setpoints for the autonomous motorcycle are denoted by $\mathbf{x_d} = [x_1^d, \ldots, , x_6^d]$. Tracking of this trajectory is achieved after applying the control input u^*. At every time instant the control input u^* is assumed to differ from the control input u appearing in Eq. (7.81) by an amount equal to Δu, that is $u^* = u + \Delta u$

$$\dot{x}_d = Ax_d + Bu^* + d_2 \tag{7.82}$$

The joint kinematics and dynamics of the riderless motorcycle is described in Eq. (7.81) can be also written as

$$\dot{x} = Ax + Bu + Bu^* - Bu^* + d_1 \tag{7.83}$$

and by denoting $d_3 = -Bu^* + d_1$ as an aggregate disturbance term one obtains

$$\dot{x} = Ax + Bu + Bu^* + d_3 \tag{7.84}$$

By subtracting Eq. (7.82) from Eq. (7.84) one has

$$\dot{x} - \dot{x}_d = A(x - x_d) + Bu + d_3 - d_2 \tag{7.85}$$

By denoting the tracking error as $e = x - x_d$ and the aggregate disturbance term as $\tilde{d} = d_3 - d_2$, the tracking error dynamics becomes

$$\dot{e} = Ae + Bu + \tilde{d} \tag{7.86}$$

The above linearized form of the motorcycle's model can be efficiently controlled after applying an H-infinity feedback control scheme.

7.4.4.2 Min-Max Control and Disturbance Rejection

The initial nonlinear model of the riderless motorcycle is in the form

$$\dot{x} = f(x,u) \;\; x \in R^n, \;\; u \in R^m \tag{7.87}$$

Linearization of the joint kinematic and dynamic model of the autonomous two-wheel vehicle is performed at each iteration of the control algorithm round its present operating point $(x^*, u^*) = (x(t), u(t - T_s))$. The linearized equivalent model of the system is described by

$$\dot{x} = Ax + Bu + L\tilde{d} \;\; x \in R^n, \;\; u \in R^m, \;\; \tilde{d} \in R^q \tag{7.88}$$

where matrices A and B are obtained from the computation of the motorcycle's Jacobians, according to Eqs. (7.76), (7.77) and (7.78) and vector $\tilde{d}$ denotes disturbance terms due to linearization errors. The problem of disturbance rejection for the linearized model that is described by

$$\begin{gathered} \dot{x} = Ax + Bu + L\tilde{d} \\ y = Cx \end{gathered} \tag{7.89}$$

where $x \in R^n$, $u \in R^m$, $\tilde{d} \in R^q$ and $y \in R^p$, cannot be handled efficiently if the classical LQR control scheme is applied. This is because of the existence of the perturbation term $\tilde{d}$. The disturbance term $\tilde{d}$ apart from modeling (parametric) uncertainty and external perturbation terms can also represent noise terms of any distribution.

In the H_∞ control approach, a feedback control scheme is designed for trajectory tracking by the autonomous motorcycle's state vector and simultaneous disturbance rejection, considering that the disturbance affects the system in the worst possible manner. The disturbances' effect are incorporated in the following quadratic cost function:

$$J(t) = \tfrac{1}{2}\int_0^T [y^T(t)y(t) + ru^T(t)u(t) - \rho^2 \tilde{d}^T(t)\tilde{d}(t)]dt, \;\; r, \rho > 0 \tag{7.90}$$

As explained in the application of the H-infinity control presented in the previous sections, the significance of the negative sign in the cost function's term that is associated with the perturbation variable $\tilde{d}(t)$ is that the disturbance tries to maximize the cost function $J(t)$ while the control signal $u(t)$ tries to minimize it. The physical meaning of the relation given above is that the control signal and the disturbances compete to each other within a min-max differential game. This problem of min-max optimization can be written as

$$min_u max_{\tilde{d}} J(u, \tilde{d}) \tag{7.91}$$

The objective of the optimization procedure is to compute a control signal $u(t)$ which can compensate for the worst possible disturbance, that is externally imposed to the system of the two-wheel autonomous vehicle. However, the solution to the min-max optimization problem is directly related to the value of the parameter ρ. This means that there is an upper bound in the disturbances magnitude that can be annihilated by the control signal.

7.4.4.3 H-Infinity Feedback Control

For the linearized system given by Eq. (7.89) the cost function of Eq. (7.90) is defined, where the coefficient r determines the penalization of the control input and the weight coefficient ρ determines the reward of the disturbances' effects. It is assumed that (i) The energy that is transferred from the disturbances signal $\tilde{d}(t)$ is bounded, that is $\int_0^\infty \tilde{d}^T(t)\tilde{d}(t)dt < \infty$, (ii) matrices $[A, B]$ and $[A, L]$ are stabilizable, (iii) matrix $[A, C]$ is detectable. Then, the optimal feedback control law is given by

$$u(t) = -Kx(t) \tag{7.92}$$

with

$$K = \frac{1}{r}B^T P \tag{7.93}$$

where P is a positive semi-definite symmetric matrix which is obtained from the solution of the Riccati equation

$$A^T P + PA + Q - P\left(\frac{1}{r}BB^T - \frac{1}{2\rho^2}LL^T\right)P = 0 \tag{7.94}$$

where Q is also a positive definite symmetric matrix. The worst case disturbance is given by

$$\tilde{d}(t) = \frac{1}{\rho^2}L^T Px(t) \tag{7.95}$$

The diagram of the considered control loop is depicted in Fig. 7.30.

7.4.5 Lyapunov Stability Analysis

Through Lyapunov stability analysis it will be shown that the proposed nonlinear control scheme assures H_∞ tracking performance for the control loop of the riderless motorcycle. Moreover, under moderate conditions asymptotic stability is proven and convergence to the reference setpoints is achieved. The tracking error dynamics for the autonomous motorcycle is written in the form

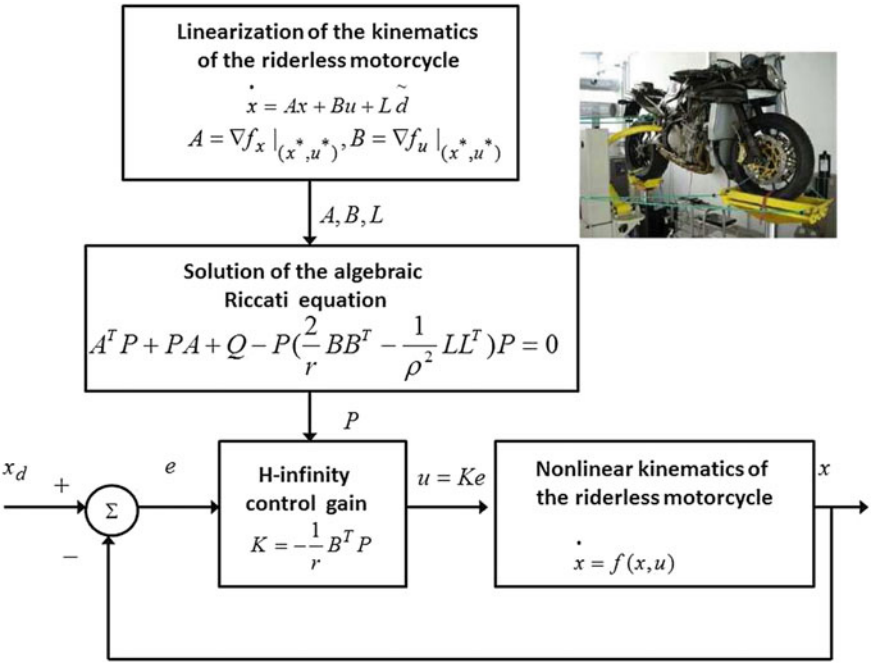

Fig. 7.30 Diagram of the nonlinear optimal control scheme for the 2-wheel autonomous vehicle (riderless motorcycle)

$$\dot{e} = Ae + Bu + L\tilde{d} \tag{7.96}$$

where in the motorcycle's case $L = I \in R^{7\times 7}$ with I being the identity matrix. Variable $\tilde{d}$ denotes model uncertainties and external disturbances of the vehicle's model. The following Lyapunov function is considered

$$V = \tfrac{1}{2}e^T Pe \tag{7.97}$$

where $e = x - x_d$ is the tracking error. By differentiating with respect to time one obtains

$$\begin{gathered} \dot{V} = \tfrac{1}{2}\dot{e}^T Pe + \tfrac{1}{2}eP\dot{e} \Rightarrow \\ \dot{V} = \tfrac{1}{2}[Ae + Bu + L\tilde{d}]^T P + \tfrac{1}{2}e^T P[Ae + Bu + L\tilde{d}] \Rightarrow \end{gathered} \tag{7.98}$$

$$\begin{gathered} \dot{V} = \tfrac{1}{2}[e^T A^T + u^T B^T + \tilde{d}^T L^T]Pe + \\ + \tfrac{1}{2}e^T P[Ae + Bu + L\tilde{d}] \Rightarrow \end{gathered} \tag{7.99}$$

$$\begin{gathered}\dot{V} = \tfrac{1}{2}e^T A^T Pe + \tfrac{1}{2}u^T B^T Pe + \tfrac{1}{2}\tilde{d}^T L^T Pe + \\ \tfrac{1}{2}e^T PAe + \tfrac{1}{2}e^T PBu + \tfrac{1}{2}e^T PL\tilde{d}\end{gathered} \tag{7.100}$$

The previous equation is rewritten as

$$\begin{gathered}\dot{V} = \tfrac{1}{2}e^T(A^T P + PA)e + \left(\tfrac{1}{2}u^T B^T Pe + \tfrac{1}{2}e^T PBu\right) + \\ + \left(\tfrac{1}{2}\tilde{d}^T L^T Pe + \tfrac{1}{2}e^T PL\tilde{d}\right)\end{gathered} \tag{7.101}$$

Assumption: For given positive definite matrix Q and coefficients r and ρ there exists a positive definite matrix P, which is the solution of the following matrix equation

$$A^T P + PA = -Q + P\left(\tfrac{2}{r}BB^T - \tfrac{1}{\rho^2}LL^T\right)P \tag{7.102}$$

Moreover, the following feedback control law is applied to the system

$$u = -\tfrac{1}{r}B^T Pe \tag{7.103}$$

By substituting Eqs. (7.102) and (7.103) one obtains

$$\begin{gathered}\dot{V} = \tfrac{1}{2}e^T\left[-Q + P\left(\tfrac{2}{r}BB^T - \tfrac{1}{2\rho^2}LL^T\right)P\right]e + \\ + e^T PB\left(-\tfrac{1}{r}B^T Pe\right) + e^T PL\tilde{d} \Rightarrow\end{gathered} \tag{7.104}$$

$$\begin{gathered}\dot{V} = -\tfrac{1}{2}e^T Qe + \left(\tfrac{2}{r}PBB^T Pe - \tfrac{1}{2\rho^2}e^T PLL^T\right)Pe \\ -\tfrac{1}{r}\left(e^T PBB^T Pe\right) + e^T PL\tilde{d}\end{gathered} \tag{7.105}$$

which after intermediate operations gives

$$\dot{V} = -\tfrac{1}{2}e^T Qe - \tfrac{1}{2\rho^2}e^T PLL^T Pe + e^T PL\tilde{d} \tag{7.106}$$

or, equivalently

$$\begin{gathered}\dot{V} = -\tfrac{1}{2}e^T Qe - \tfrac{1}{2\rho^2}e^T PLL^T Pe + \\ + \tfrac{1}{2}e^T PL\tilde{d} + \tfrac{1}{2}\tilde{d}^T L^T Pe\end{gathered} \tag{7.107}$$

Lemma: The following inequality holds

$$\tfrac{1}{2}e^T L\tilde{d} + \tfrac{1}{2}\tilde{d}L^T Pe - \tfrac{1}{2\rho^2}e^T PLL^T Pe \leq \tfrac{1}{2}\rho^2\tilde{d}^T\tilde{d} \tag{7.108}$$

Proof: The binomial $(\rho\alpha - \frac{1}{\rho}b)^2$ is considered. Expanding the left part of the above inequality one gets

$$\begin{gathered}\rho^2 a^2 + \tfrac{1}{\rho^2}b^2 - 2ab \geq 0 \Rightarrow \tfrac{1}{2}\rho^2 a^2 + \tfrac{1}{2\rho^2}b^2 - ab \geq 0 \Rightarrow \\ ab - \tfrac{1}{2\rho^2}b^2 \leq \tfrac{1}{2}\rho^2 a^2 \Rightarrow \tfrac{1}{2}ab + \tfrac{1}{2}ab - \tfrac{1}{2\rho^2}b^2 \leq \tfrac{1}{2}\rho^2 a^2\end{gathered} \tag{7.109}$$

The following substitutions are carried out: $a = \tilde{d}$ and $b = e^T PL$ and the previous relation becomes

$$\frac{1}{2}\tilde{d}^T L^T Pe + \frac{1}{2}e^T PL\tilde{d} - \frac{1}{2\rho^2}e^T PLL^T Pe \leq \frac{1}{2}\rho^2 \tilde{d}^T \tilde{d} \tag{7.110}$$

Equation (7.110) is substituted in Eq. (7.107) and the inequality is enforced, thus giving

$$\dot{V} \leq -\frac{1}{2}e^T Qe + \frac{1}{2}\rho^2 \tilde{d}^T \tilde{d} \tag{7.111}$$

Equation (7.111) shows that the H_∞ tracking performance criterion is satisfied. The integration of $\dot{V}$ from 0 to T gives

$$\begin{gathered} \int_0^T \dot{V}(t)dt \leq -\frac{1}{2}\int_0^T ||e||_Q^2 dt + \frac{1}{2}\rho^2 \int_0^T ||\tilde{d}||^2 dt \Rightarrow \\ 2V(T) + \int_0^T ||e||_Q^2 dt \leq 2V(0) + \rho^2 \int_0^T ||\tilde{d}||^2 dt \end{gathered} \tag{7.112}$$

Moreover, if there exists a positive constant $M_d > 0$ such that

$$\int_0^\infty ||\tilde{d}||^2 dt \leq M_d \tag{7.113}$$

then one gets

$$\int_0^\infty ||e||_Q^2 dt \leq 2V(0) + \rho^2 M_d \tag{7.114}$$

Thus, the integral $\int_0^\infty ||e||_Q^2 dt$ is bounded. Moreover, $V(T)$ is bounded and from the definition of the Lyapunov function V in Eq. (7.97) it becomes clear that $e(t)$ will be also bounded since $e(t) \in \Omega_e = \{e | e^T Pe \leq 2V(0) + \rho^2 M_d\}$. According to the above and with the use of Barbalat's Lemma one obtains $lim_{t\to\infty} e(t) = 0$.

Elaborating on the above, it can be noted that the proof of global asymptotic stability for the control loop of the autonomous motorcycle is based on Eq. (7.111) and on the application of Barbalat's Lemma. It uses the condition of Eq. (7.113) about the boundedness of the square of the aggregate disturbance and modelling error term $\tilde{d}$ that affects the model. However, as explained above the proof of global asymptotic stability is not restricted by this condition. By selecting the attenuation coefficient ρ to be sufficiently small and in particular to satisfy $\rho^2 < ||e||_Q^2 / ||\tilde{d}||^2$ one has that the first derivative of the Lyapunov function is upper bounded by 0. Therefore for the ith time interval it is proven that the Lyapunov function defined in Eq. (7.97) is a decreasing one. This also assures the Lyapunov function of the system defined in Eq. (7.97) will always have a negative first-order derivative.

7.4.6 Robust State Estimation with the Use of the H-Infinity Kalman Filter

The control loop for the autonomous motorcycle can be implemented with the feedback of a partially measurable state vector and by processing only a small number of state variables. To reconstruct the missing information about the state vector of the autonomous two-wheel vehicle it is proposed to use a filtering scheme which allows to apply state estimation-based control [457]. The recursion of the H_∞ Kalman Filter, for the model of the distributed finance agents, can be formulated in terms of a *measurement update* and a *time update* part

Measurement update:

$$\begin{aligned} D(k) &= [I - \theta W(k)P^{-}(k) + C^{T}(k)R(k)^{-1}C(k)P^{-}(k)]^{-1} \\ K(k) &= P^{-}(k)D(k)C^{T}(k)R(k)^{-1} \\ \hat{x}(k) &= \hat{x}^{-}(k) + K(k)[y(k) - C\hat{x}^{-}(k)] \end{aligned} \tag{7.115}$$

Time update:

$$\begin{aligned} \hat{x}^{-}(k+1) &= A(k)x(k) + B(k)u(k) \\ P^{-}(k+1) &= A(k)P^{-}(k)D(k)A^{T}(k) + Q(k) \end{aligned} \tag{7.116}$$

where it is assumed that parameter θ is sufficiently small to assure that the covariance matrix $P^{-}(k)^{-1} - \theta W(k) + C^{T}(k)R(k)^{-1}C(k)$ will be positive definite. When $\theta = 0$ the H_∞ Kalman Filter becomes equivalent to the standard Kalman Filter. One can measure only a part of the state vector of the system of the autonomous motorcycle, such as the cartesian coordinates of its rear wheels (x, y) and can estimate through filtering the rest of the state vector elements.

7.4.7 Simulation Tests

The performance of the proposed nonlinear optimal (H-infinity) control method for the model of the autonomous motorcycle has been tested through simulation experiments. The simulation results depicted in Figs. 7.31, 7.32, 7.33, 7.34, 7.35, 7.36, 7.37 and 7.38 confirm the stability properties of the control loop that was previously proven through Lyapunov analysis. Moreover, they demonstrate that the state vector elements of the motorcycle could track precisely the reference setpoints and that the two-wheel vehicle could follow accurately the designated paths in the 2D motion plane. This comes to point out that under electronic control, several of the motorcycle's driving tasks such as lane following, lane change or vehicle overtaking can be safely performed. The implementation of the proposed control scheme required the solution at each time step of the algebraic Riccati equation, given in Eq. (7.102).

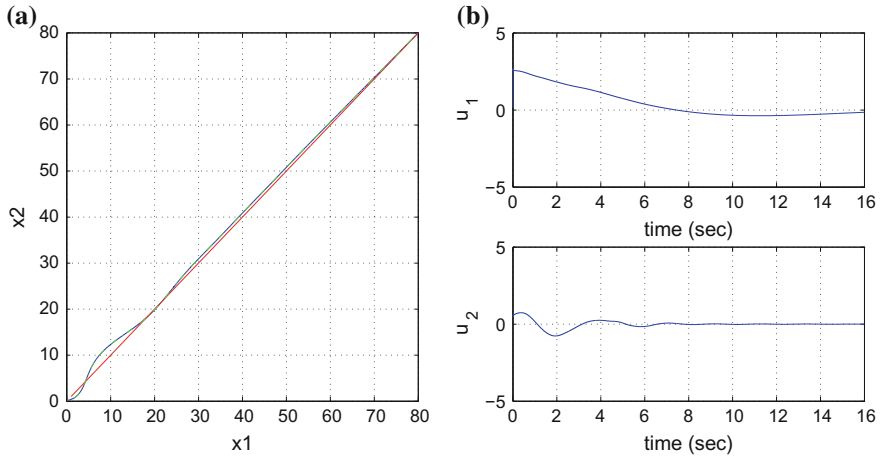

Fig. 7.31 **a** Tracking of reference path 1 (red-line) by the autonomous motorcycle (blue line) and trajectory estimated by the Kalman Filter (green line), **b** control inputs u_1 to u_2 applied to the autonomous motorcycle

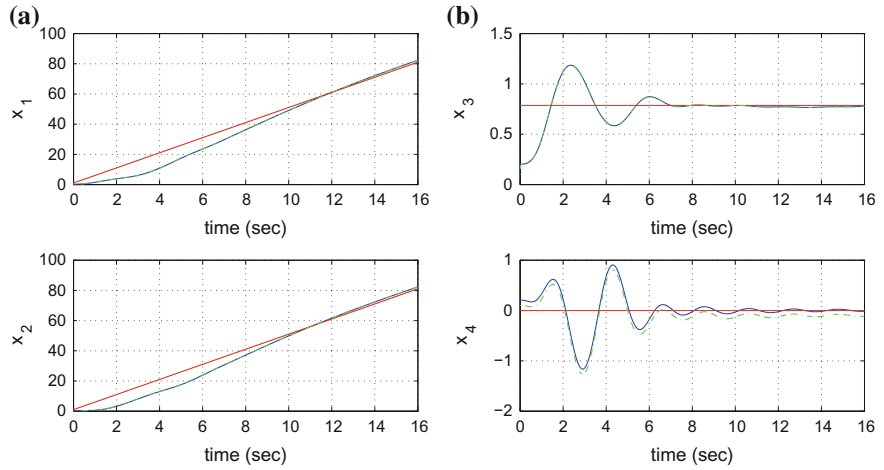

Fig. 7.32 Tracking of reference path 1: **a** convergence of state variables x_1 to x_2 of the autonomous motorcycle to their reference setpoints (red-lines) and estimated state variables provided by the Kalman Filter (green lines), **b** convergence of state variables x_3 to x_4 of the autonomous motorcycle to their reference setpoints (red-lines) and estimated state variables provided by the Kalman Filter (green lines)

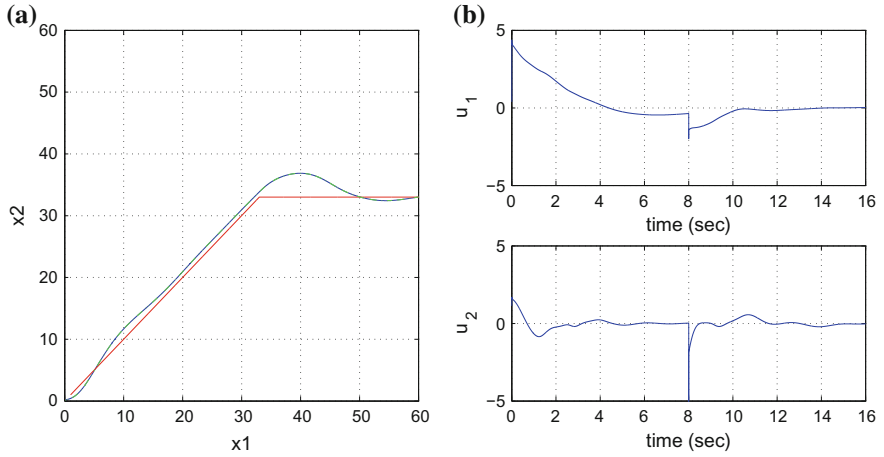

Fig. 7.33 **a** Tracking of reference path 2 (red-line) by the autonomous motorcycle (blue line) and trajectory estimated by the Kalman Filter (green line), **b** control inputs u_1 to u_2 applied to the autonomous motorcycle

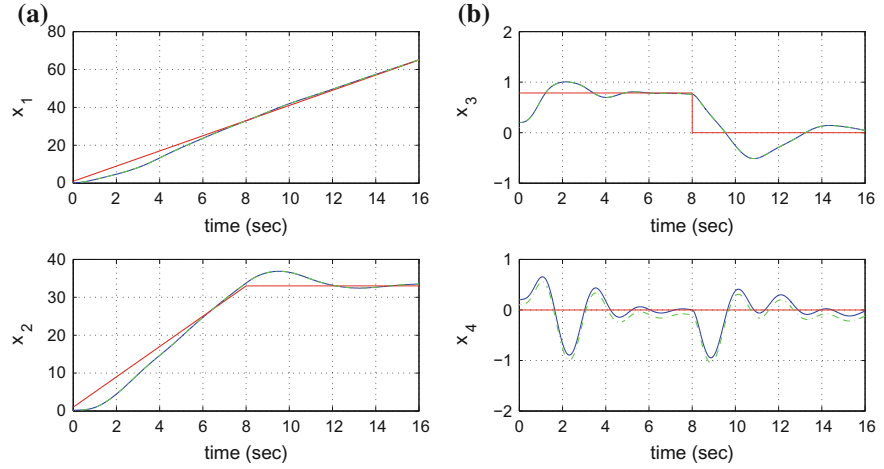

Fig. 7.34 Tracking of reference path 2: **a** convergence of state variables x_1 to x_2 of the autonomous motorcycle to their reference setpoints (red-lines) and estimated state variables provided by the Kalman Filter (green lines), **b** convergence of state variables x_3 to x_4 of the autonomous motorcycle to their reference setpoints (red-lines) and estimated state variables provided by the Kalman Filter (green lines)

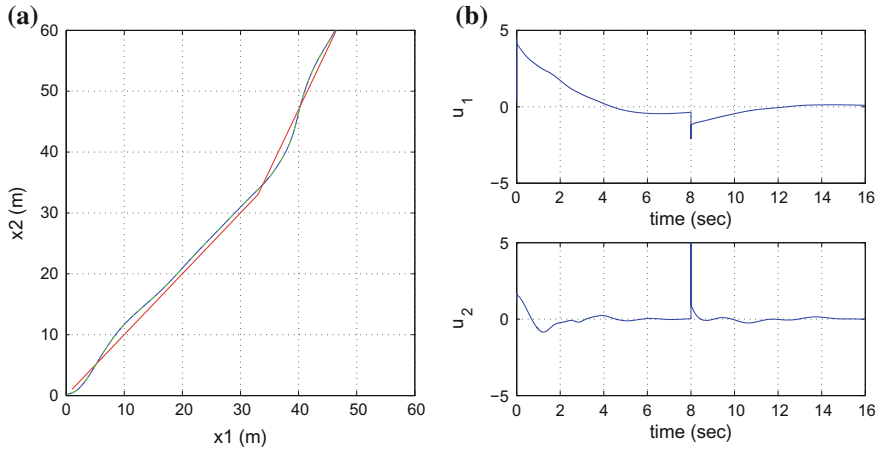

Fig. 7.35 **a** Tracking of reference path 3 (red-line) by the autonomous motorcycle (blue line) and trajectory estimated by the Kalman Filter (green line), **b** control inputs u_1 to u_2 applied to the autonomous motorcycle

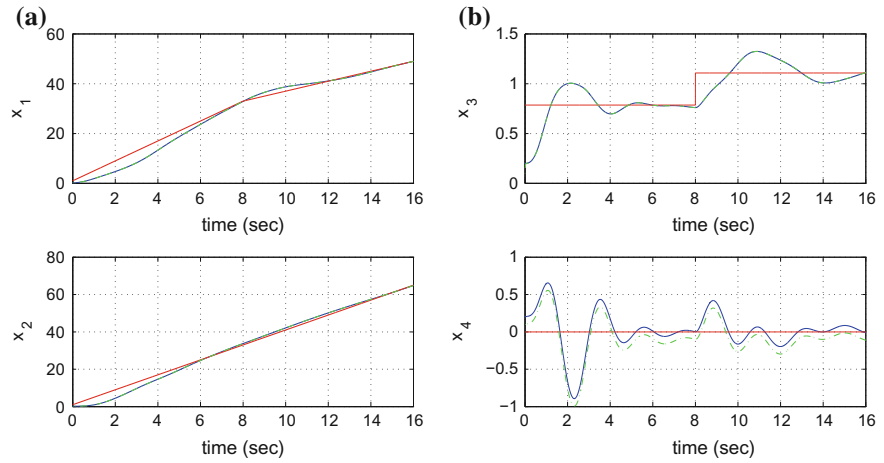

Fig. 7.36 Tracking of reference path 3: **a** convergence of state variables x_1 to x_2 of the autonomous motorcycle to their reference setpoints (red-lines) and estimated state variables provided by the Kalman Filter (green lines), **b** convergence of state variables x_3 to x_4 of the autonomous motorcycle to their reference setpoints (red-lines) and estimated state variables provided by the Kalman Filter (green lines)

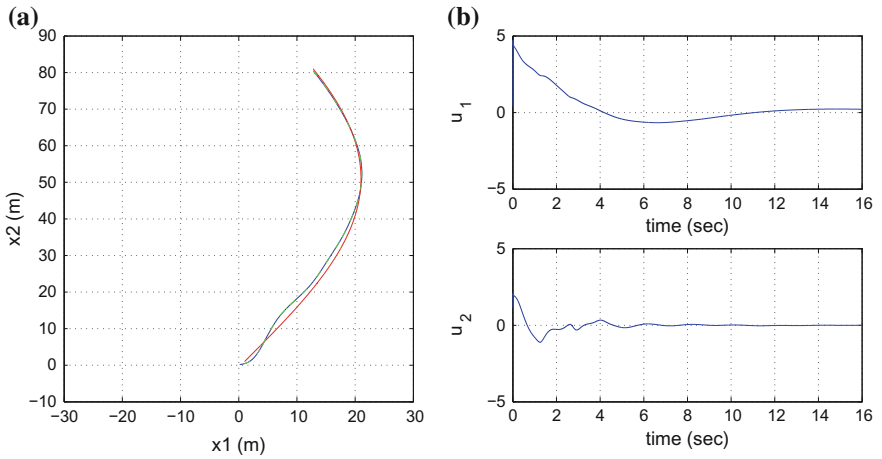

Fig. 7.37 **a** Tracking of reference path 4 (red-line) by the autonomous motorcycle (blue line) and trajectory estimated by the Kalman Filter (green line), **b** control inputs u_1 to u_2 applied to the autonomous motorcycle

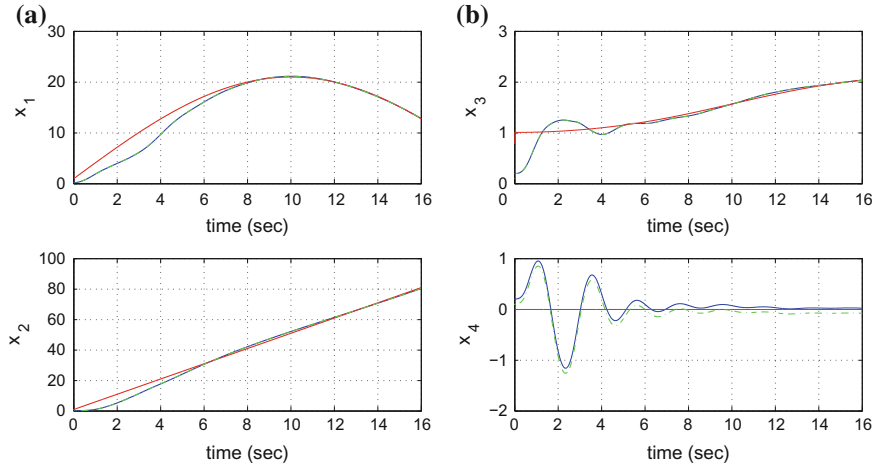

Fig. 7.38 Tracking of reference path 4: **a** convergence of state variables x_1 to x_2 of the autonomous motorcycle to their reference setpoints (red-lines) and estimated state variables provided by the Kalman Filter (green lines), **b** convergence of state variables x_3 to x_4 of the autonomous motorcycle to their reference setpoints (red-lines) and estimated state variables provided by the Kalman Filter (green lines)

To implement state estimation-based control from the autonomous motorcycle through the processing of a small number of on-board sensor measurements, the H-infinity Kalman filter has been used as a robust state estimator. Actually, it was necessary to receive measurements about the cartesian coordinates (x, y) of the vehicle's rear wheel, while the rest of the state vector elements of the motorcycle could be estimated through the H-infinity Kalman Filter. In the simulation diagrams, the real values of the state vector components of the two-wheel vehicle are depicted in blue colour, the estimated values are plotted in green while the associated reference setpoints are printed in red colour. It can be noted that the proposed control method achieved fast and accurate tracking of the reference setpoints, while the variations of the control inputs remained smooth and moderate.

Despite its computational simplicity, the proposed H_∞ control scheme has an excellent performance. Comparing to the control of autonomous vehicles that rely on global linearization methods the presented nonlinear H-infinity control scheme is equally efficient in setpoint tracking while also retaining optimal control features [457]. The tracking accuracy of the presented control method (H_∞) has been monitored in the case of several reference setpoints. By using the Kalman Filter as a robust observer estimates of the state vector of the two-wheel vehicle were obtained thus the implementation of state estimation-based control became possible. The measured state variables were $x_1 = x$, $x_2 = y$. It can be noticed that despite model perturbations the tracking accuracy of the control method remained satisfactory. The RMSE of the tracking reference setpoints by the state variables of the motorcycle is given in Table 7.1. Moreover, the tracking performance of the nonlinear H-infinity control method for the model of the autonomous motorcycle was measured in the case of model uncertainty, imposing an imprecision equal to $\Delta a\%$ about the vehicle's mass m. The obtained results are outlined in Table 7.2. It can be noticed that despite model perturbations the tracking accuracy of the control method remained satisfactory (Tables 7.3 and 7.4).

Table 7.2 Tracking RMSE in motion under disturbances

	$RMSE_x$	$RMSE_y$	$RMSE_\theta$
Path_1	$37.00 \cdot 10^{-4}$	$54.00 \cdot 10^{-4}$	$13.00 \cdot 10^{-4}$
Path_2	$14.00 \cdot 10^{-4}$	$16.00 \cdot 10^{-4}$	$2.41 \cdot 10^{-4}$

Table 7.3 RMSE of the autonomous motorcycle's state variables

Path	RMSE X (m)	RMSE Y (m)	RMSE ψ (rad)	RMSE ϕ (rad)
1	$2.5 \cdot 10^{-3}$	$11.3 \cdot 10^{-3}$	$0.1 \cdot 10^{-3}$	$0.3 \cdot 10^{-3}$
2	$4.8 \cdot 10^{-3}$	$19.7 \cdot 10^{-3}$	$3.0 \cdot 10^{-3}$	$3.2 \cdot 10^{-3}$
3	$1.4 \cdot 10^{-3}$	$6.6 \cdot 10^{-3}$	$0.7 \cdot 10^{-3}$	$1.1 \cdot 10^{-3}$
4	$1.9 \cdot 10^{-3}$	$26.3 \cdot 10^{-3}$	$0.1 \cdot 10^{-3}$	$1.2 \cdot 10^{-3}$

Table 7.4 RMSE of the motorcycle under disturbance

Δa (%)	RMSE X (m)	RMSE Y (m)	RMSE ψ (rad)	RMSE ϕ (rad)
0	$1.9{\cdot}10^{-3}$	$26.3{\cdot}10^{-3}$	$0.1{\cdot}10^{-3}$	$1.2{\cdot}10^{-3}$
10	$1.9{\cdot}10^{-3}$	$26.3{\cdot}10^{-3}$	$0.1{\cdot}10^{-3}$	$1.2{\cdot}10^{-3}$
20	$1.2{\cdot}10^{-3}$	$23.4{\cdot}10^{-3}$	$0.2{\cdot}10^{-3}$	$1.1{\cdot}10^{-3}$
30	$2.4{\cdot}10^{-3}$	$26.9{\cdot}10^{-3}$	$0.1{\cdot}10^{-3}$	$1.3{\cdot}10^{-3}$
40	$3.7{\cdot}10^{-3}$	$16.0{\cdot}10^{-3}$	$0.1{\cdot}10^{-3}$	$0.7{\cdot}10^{-3}$
50	$4.0{\cdot}10^{-3}$	$16.0{\cdot}10^{-3}$	$0.2{\cdot}10^{-3}$	$0.8{\cdot}10^{-3}$
60	$8.5{\cdot}10^{-3}$	$17.1{\cdot}10^{-3}$	$0.5{\cdot}10^{-3}$	$2.3{\cdot}10^{-3}$